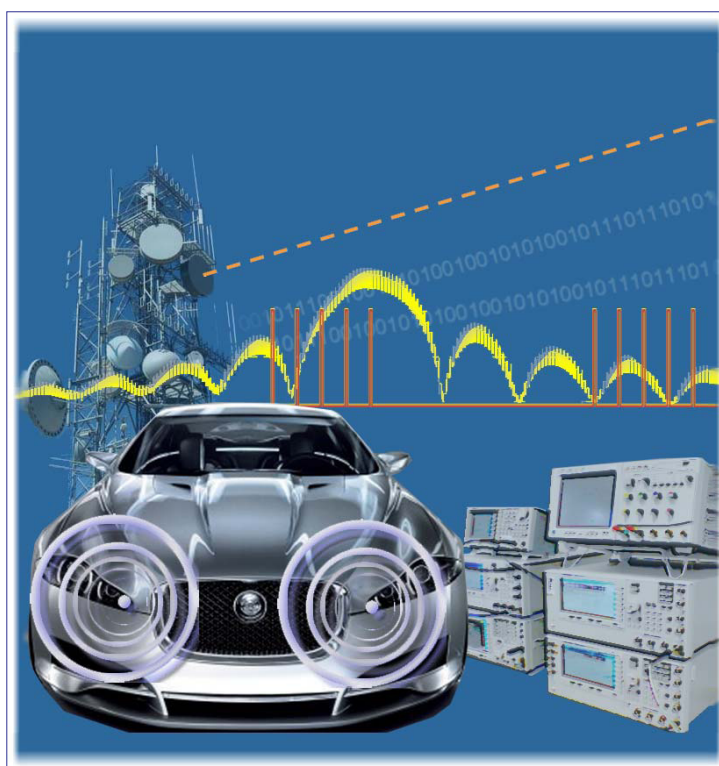


Interference from Low-Duty Cycle 26 GHz Automotive Short Range Radar (SRR)

Assessment of the effect of Low-Duty Cycle operation on the interference from Automotive Short Range Radar(SRR) on licensed Fixed Wireless services in the 24.25-26.65GHz band

D.Fuehrer, E. Cano-Pons, J. Fortuny-Guasch



EUR 24833 EN

The mission of the IPSC is to provide research results and to support EU policy-makers in their effort towards global security and towards protection of European citizens from accidents, deliberate attacks, fraud and illegal actions against EU policies

European Commission
Joint Research Centre
Institute for the Protection and Security of the Citizen

Contact information

Address: Via E. Fermi 2749, 21027 Ispra (VA), Italy
E-mail: Joaquim.Fortuny@jrc.ec.europa.eu
Tel.: +39 0332 785104
Fax: +39 0332 786565

<http://ipsc.jrc.ec.europa.eu/>
<http://www.jrc.ec.europa.eu/>

Legal Notice

Neither the European Commission nor any person acting on behalf of the Commission is responsible for the use which might be made of this publication.

Disclaimer

Certain commercial equipment and software are identified in this study to specify technical aspects of the reported results. In no case such identification does imply recommendation or endorsement by the European Commission Joint Research Centre, nor does imply that the equipment identified is necessarily the best available for the purpose.

**Europe Direct is a service to help you find answers
to your questions about the European Union**

Freephone number (*): 00 800 6 7 8 9 10 11

(*) Certain mobile telephone operators do not allow access to 00 800 numbers or these calls may be billed.

A great deal of additional information on the European Union is available on the Internet. It can be accessed through the Europa server <http://europa.eu/>

JRC64739

EUR 24833 EN
ISBN 978-92-79-20396-1 (print)
ISBN 978-92-79-20397-8 (pdf)

ISSN 1018-5593 (print)
ISSN 1831-9424 (online)

doi:10.2788/24368

Luxembourg: Publications Office of the European Union

© European Union, 2011

Reproduction is authorised provided the source is acknowledged
Printed in Italy

Table of contents

GLOSSARY	2
1. INTRODUCTION	3
2. TEST CONCEPT	4
3. SIGNAL CHARACTERISTICS	6
3.1 INTERFERING SIGNAL.....	6
3.2 VICTIM SIGNAL	7
4. TEST SCENARIOS	9
4.1 SINGLE-SOURCE INTERFERENCE	9
4.2 AGGREGATE INTERFERENCE	9
5. MEASUREMENTS	11
5.1 SETUP AND SIGNAL GENERATION	11
5.2 MEASUREMENT RESULTS – SINGLE-SOURCE INTERFERENCE	15
5.3 MEASUREMENT RESULTS - AGGREGATE INTERFERENCE	20
5.4 SIMULATION RESULTS – SUMMARY.....	23
6. SUMMARY AND CONCLUSION	24
ANNEX A – SIMULATION REPORT	25
A.1 EVALUATION METRICS	25
A.2 SYSTEM MODEL	26
A.3 SIMULATION ANALYSIS	29
A.3.1 <i>Single Interferer</i>	29
A.3.2 <i>Aggregate Interference Effects</i>	30
REFERENCES	50
NORMATIVE REFERENCES	50
INFORMATIVE REFERENCES	51

Glossary

ADC	Analogue-To-Digital Converter
AF	Activity Factor
AWGN	Additive White Gaussian Noise
BER	Bit Error Rate
BPSK	Binary Phase-Shift Keying
CEPT	European Conference of Postal and Telecommunications Administrations
DAC	Digital-To-Analogue Conversion
DC	Duty Cycle
DS-UWB	Direct Sequence Ultra Wideband
EC	European Commission
ECC	Electronic Communications Committee
EVM	Error Vector Magnitude
FDD	Frequency Division Duplex
FH-UWB	Frequency Hopping Ultra Wideband
FS	Fixed System
I/N	Interference-to-Noise
LDC	Low Duty Cycle
LOS	Line Of Sight
NIR	Noise-to-Interference Ratio
PAR	Peak-to-Average Ratio
PF	Penetration Factor
PRF	Pulse Repetition Frequency
PRI	Pulse Repetition Interval
PSD	Power Spectral Density
PTP	Point-To-Point
QAM	Quadrature Amplitude Modulation
QPSK	Quadrature Phase-Shift Keying
RF	Radio Frequency
RMS	Root Mean Square
SINR	Signal-to-Interference-plus-Noise Ratio
SNR	Signal-to-Noise Ratio
SRR	Short Range Radar
UWB	Ultra Wideband

1. Introduction

Currently, there are two frequency bands allocated to Ultra-Wideband (UWB) automotive short range radar (SRR) equipment in Europe. In its Decision 2005/50/EC of 17 January 2005 [1] the European Commission (EC) designated the frequency band 21.65-26.65 GHz (referred to as the “24 GHz band”) for use until mid 2013. The frequency band 77-81 GHz (the “79 GHz band”) has been designated and made available for permanent usage by EC Decision 2004/545/EC of 8 July 2004 [2]. In order to ease the transition from 24 GHz to 79 GHz technology the EC considers authorizing the use of a band in the 24 GHz range for SRR beyond 2013. In Report 37 of the European Conference of Postal and Telecommunications Administrations (CEPT) [3] which was prepared in response to the “SRR mandate 2” issued by the EC to the CEPT it is proposed to allocate the frequency band 24.25 – 27.50 GHz (the “26 GHz band”) to SRR and reduce the risk of interference to licensed services operating in the same band through lower transmit power limits and low duty cycle (LDC) operation. As this proposal was not accepted the discussion now centres on the frequency band 24.25 – 26.65 GHz (the “revised 26 GHz band”).

The objective of this report is to complement the very detailed and comprehensive compatibility studies that have been undertaken by CEPT, ITU-R, ETSI, and other institutions over the past years by evaluating the impact of LDC on the level of interference generated by automotive UWB SRR systems in the revised 26 GHz band. In particular, the impact on digitally modulated single carrier signals as used by licensed microwave fixed wireless links is investigated. The conclusions drawn in this report will hopefully be useful for defining the future regulation for automotive SRR in the European Union.

2. Test concept

In this study we investigate the impact of single-source and aggregate interference from pulsed UWB signals, with and without LDC, on a victim signal. The victim signal is a single-band digitally modulated signal with a carrier frequency in the 24.25-26.65 GHz range, as used by licensed point-to-point (PTP) microwave links. For this purpose we conducted a series of measurements and simulations.

Quantifying the impact of automotive UWB SRR on microwave fixed links is a very complex matter. Widely varying system characteristics, geography, weather, climate, and many other parameters have to be taken into account. Nevertheless this subject has been thoroughly researched so that we considered it unnecessary trying to reproduce previous research work.

We therefore decided to conduct a comparative study with the goal to determine the potential gain in Signal-to-Noise Ratio (SNR) achieved by applying various duty cycles to SRR-like UWB signals.

As metric for determining the quality of the victim signal we chose the error vector magnitude (EVM). While the bit error rate (BER) is the preferred parameter to verify receiver performance, the EVM is an alternative to examine the quality of a demodulated signal if measuring the BER directly is not practical or possible. The meaning of the EVM can best be understood by looking at the IQ diagram or constellation of a digitally modulated signal. In Figure 1 two versions of the constellation of a 16-QAM signal are shown. Without impairment, the symbol locations are well defined (left). In the presence of noise, however, symbol locations vary according to the level of impairment (right).

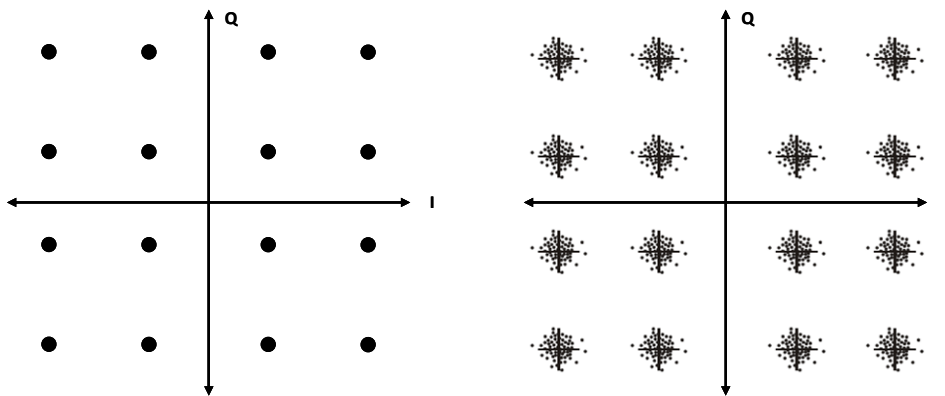
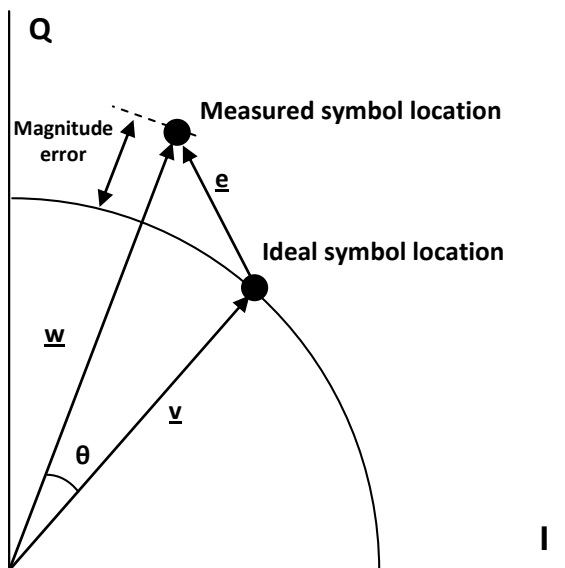


Figure 1: Constellation of a digitally modulated signal (16-QAM), ideal (left), and in the presence of noise (right)

The soft symbol decisions obtained after decimating the recovered waveform at the demodulator output are compared against the ideal symbol locations (Figure 2). The root mean square (RMS) error vector magnitude and phase error are then used in determining the EVM measurement over a window of a certain number of demodulated symbols.



- \underline{v} : Ideal symbol vector
- \underline{w} : Measured symbol vector
- $\underline{w}-\underline{v}$: Magnitude error
- θ : Phase error
- $\underline{e}=\underline{w}-\underline{v}$: Error vector

Figure 2: Error Vector Magnitude
(source: National Instruments)

To remove the dependence on system gain distribution, EVM is normalized by $|\underline{v}|$ and expressed as a percentage.

From the EVM the BER can be deducted via the SNR which can be expressed as:

$$\text{SNR [dB]} = -20 * \log (\text{EVM [\%]} / 100)$$

The relation between SNR and BER which depends on the type of modulation is well established. Generally, it is assumed that the noise "N" is Additive White Gaussian Noise (AWGN) with a finite peak-to-average ratio, while in this study we have to consider impulsive noise. Nevertheless, the EVM can provide an indication of the level of impairment to be expected.

3. Signal characteristics

3.1 Interfering signal

There are numerous modulation schemes that may be employed in automotive SRR systems, a selection of which is presented in [6] [1] . In this study we chose Pulsed Frequency Hopping (FH). Pulsed FH-UWB is considered to have a reduced interference impact compared to other pulsed UWB variants [4] and may therefore be the preferred technology for future deployments.

The basic UWB signal characteristics are shown in Table 1. The values for the “24 GHz band” [5] are provided as a reference only.

Reference	Original limits for the "24 GHz band"	Proposal for the "revised 26 GHz band"
	CEPT Report 36	DG INFSO
SRR Frequency Range	21.65-26.65 GHz (5 GHz)	24.25-26.65 GHz (2 GHz)
Mean e.i.r.p. @ 1MHz/ms	-41.3dBm/MHz	-50 dBm/MHz
Peak e.i.r.p. @ 50MHz	0 dBm	-7dBm/50MHz (for iBW ³ 50MHz) or -7dBm - 20*log(50MHz / iBW) measured with RBW = iBW (for iBW<50MHz)
Duty Cycle (DC)	No limit (up to 100%)	2% to 10% per 50MHz and per sec

Table 1: Comparison of UWB signal characteristics

The terms Pulse, Pulse width, Burst, Duty Cycle (DC), and Activity Factor (AF) illustrated in Figure 3 have been defined according to [4] .

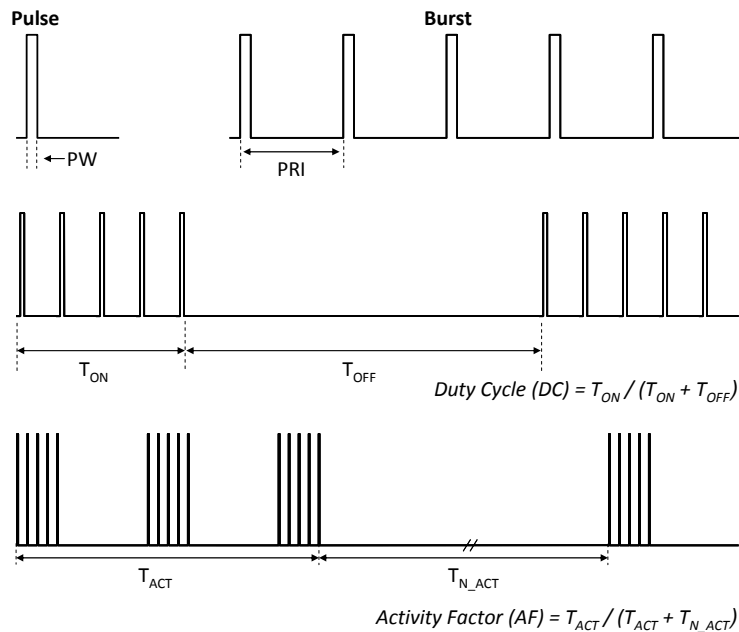


Figure 3: UWB pulse definition (based on ETSI TR 102 664 v1.2.1)

An exemplary hopping sequence of a pulsed FH-UWB signal is shown in Figure 4. The duty cycle is observed in both time and frequency domains.

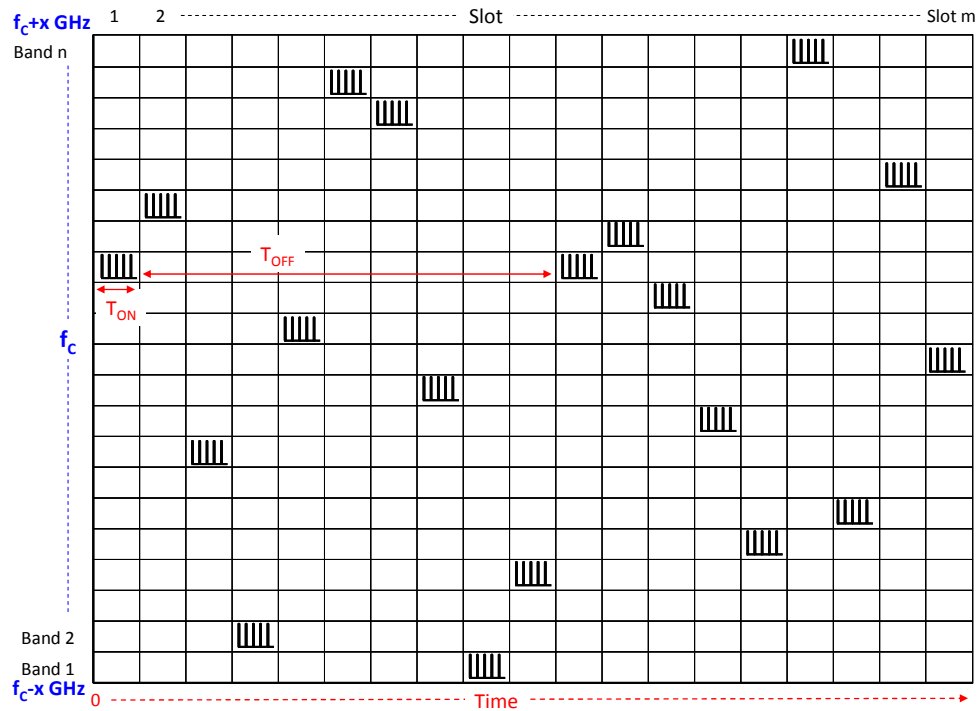


Figure 4: Exemplary hopping sequence of a pulsed FH-UWB signal with DC

3.2 Victim signal

A typical victim signal is characterized by the following parameters:

- System type: Short-range Point-to-Point (PTP) microwave link
- RF band: 26 GHz Band (24.25 – 26.5 GHz)
- Channel bandwidth: 7, 14, 28, 56 MHz
- Signal type: Single carrier
- Modulation: QPSK, 8PSK, 16 QAM, 32 QAM, 64 QAM, 128 QAM, 256 QAM-L, 256 QAM-H
- Duplexing method: FDD
- Tx/Rx channel separation: 1008 MHz

Further victim signal characteristics are described in [7].

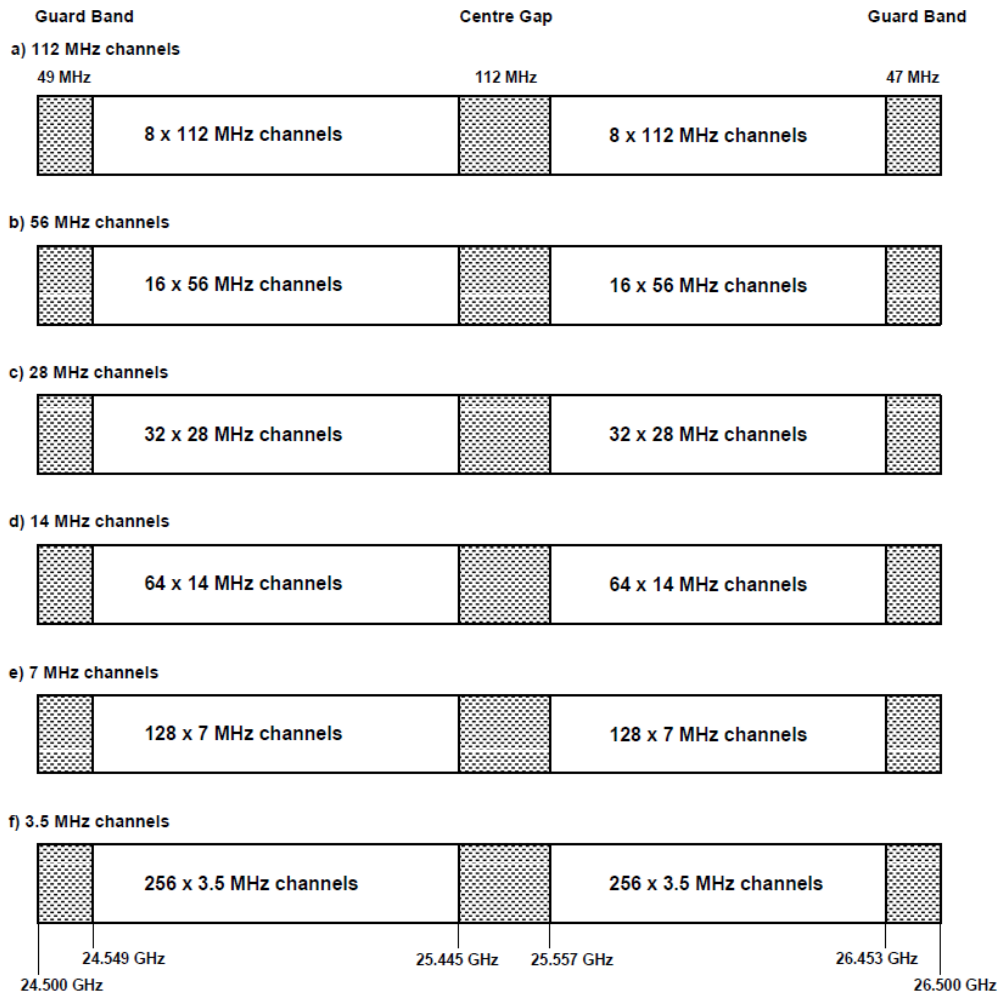


Figure 5: FS frequency allocation in the 24.5 -26.5 GHz band (source: CEPT T/R13-02)

4. Test scenarios

4.1 Single-source interference

The impact of different types of UWB pulses on the EVM of the victim signal was investigated. Pulses were transmitted continuously and with various duty cycles applied.

	Reference Pulse			"Worst case" Pulse 1		"Worst case" Pulse 2		ECC Rep. 158 Pulse 3		ECC Rep. 158 Pulse 4	
Pulse shape	Rectangular			Rectangular		Rectangular		Rectangular		Rectangular	
Single pulse bandwidth [MHz]	50			50		50		50		50	
PRI [ns]	180			800		160		10000		370	
PRF [MHz]	5,56			1,25		6,25		0,1		2,7	
Duty cycle within 50 MHz	100%	10%	2%	100%	10%	100%	2%	100%	10%	100%	10%
Burst length [μ s]	-	20		-	96	-	19,2	-	20	-	20
Cycle duration [μ s]	-	200	1.000	-	960	-	960	-	200	-	200
Burst frequency [kHz]	-	5,0	1,0	-	1,04	-	1,0	-	5,0	-	5,0

Table 2: FH-UWB pulse parameters – Single interferer scenario

The parameters of the reference pulse were chosen according to the example of an automotive SRR system provided in section B.1.2 of [4], the parameters of the other pulses match those of pulsed FH-UWB signals identified as being particularly critical in [8].

4.2 Aggregate interference

For evaluating the impact of LDC on interference generated by multiple sources a single-car entry scenario comparable to the ones defined in [8] [9] [8] and [10] was as chosen. As antenna directivity and gain were not considered we assumed a horizontal offset of zero between road and FS receiver.

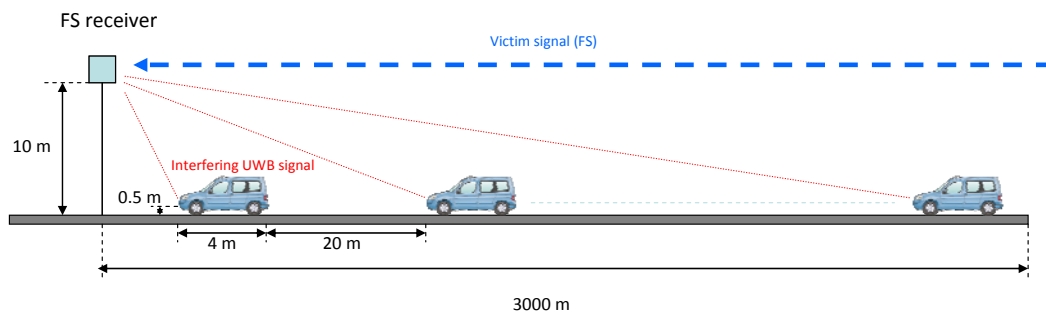


Figure 6: Aggregate interference scenario (single-car entry)

The following parameters were applied:

- Road length: 3000 m
- Car length: 4 m
- Distance between cars: 20 m
- Car height: 1.5 m
- SRR height above ground: 0.5 m
- FS receiver height: 10 m
- No. of SRR sensors per car: 2 (front)

Four market penetration scenarios were investigated, with penetration rates of 7%, 10%, 40%, and 100%. The number of cars was calculated accordingly as 9, 13, 50, and 125. In the measurements, as well as in the simulations we took worst-case assumptions, i. e. all SRR-equipped cars would be located as closely as possible to the victim receiver.

The effect of shading was taken into account according to the definition given in [9]. Bumper loss, antenna gain and directivity, rain fading and other effects have not been taken into account as they are not relevant for this comparative study.

Activity factors lower than 100% were not taken into account in this study. Studies performed by ITU-R revealed that the average activity factor is close to 50% corresponding to a reduction of the aggregate interference level of approx. 3 dB [11].

For the aggregate interference scenario three different pulse types were evaluated, operating in continuous mode and with different duty cycles.

	Pulse 1			Pulse 2		Pulse 3	
Pulse shape	Rectangular			Rectangular		Rectangular	
Single pulse bandwidth [MHz]	50			50		50	
PRI [ns]	180			800		160	
PRF [MHz]	5,556			1,25		6,25	
Burst length [μ s]	-	20		-	96	-	19,2
Duty cycle within 50 MHz	100%	10%	2%	100%	10%	100%	2%
Max. mean power [dBm/MHz]	-41,3			-41,3		-41,3	

Table 3: FH-UWB pulse parameters – Aggregate interference scenario

The parameters of Pulse 1 were chosen according to the example of an automotive SRR system provided in section B.1.2 of [4], the parameters of Pulses 2 and 3 match those of pulsed FH-UWB signals identified as being particularly critical in [8].

5. Measurements

5.1 Setup and signal generation

For reasons of flexibility both the victim and the interfering signals were generated with configurable microwave signal generators. The victim base band signal was generated with an Agilent E8267 vector signal generator and then upconverted to 26 GHz with an Agilent E8257 analogue signal generator.

The signal of the single interferer was generated with a second Agilent E8257 in stand-alone mode. For applying different duty cycles a gating signal was generated by a Tektronix AFG3251 function generator.

The aggregate interference signal was programmed in MATLAB, generated in the baseband with an Agilent N6030A Arbitrary Waveform Generator and then upconverted to 26 GHz with the E8267 and E8257 combination.

Victim and interfering signals were combined through a microwave combiner and the resulting signal was analysed using an Agilent N9030A Vector Signal Analyser.

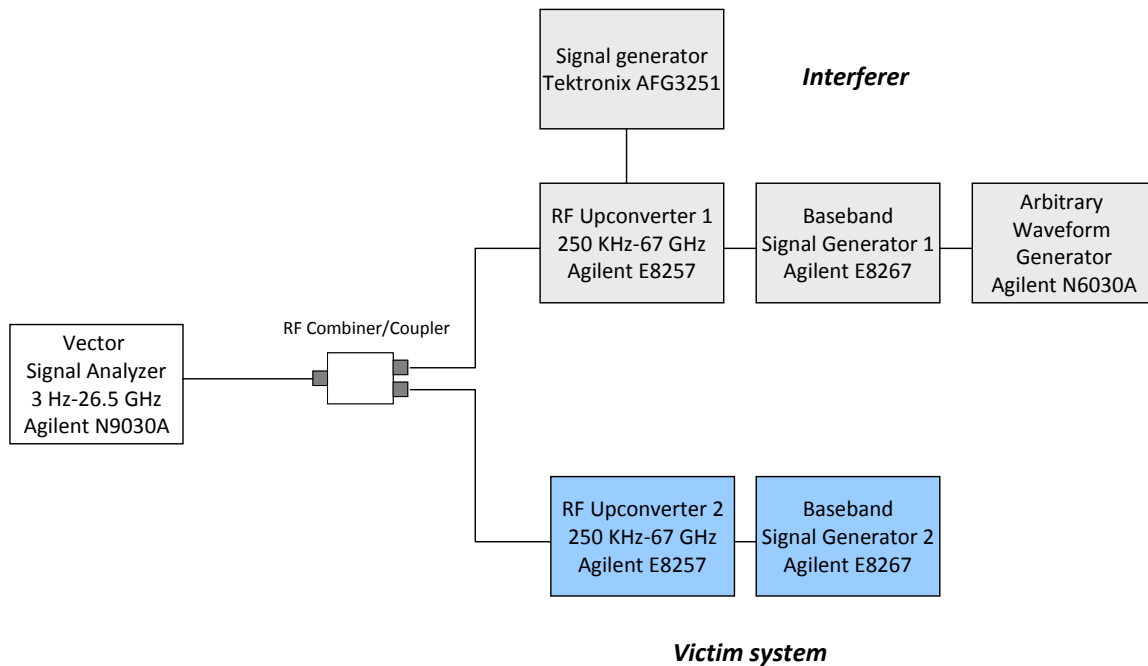


Figure 7: Measurement setup – Concept

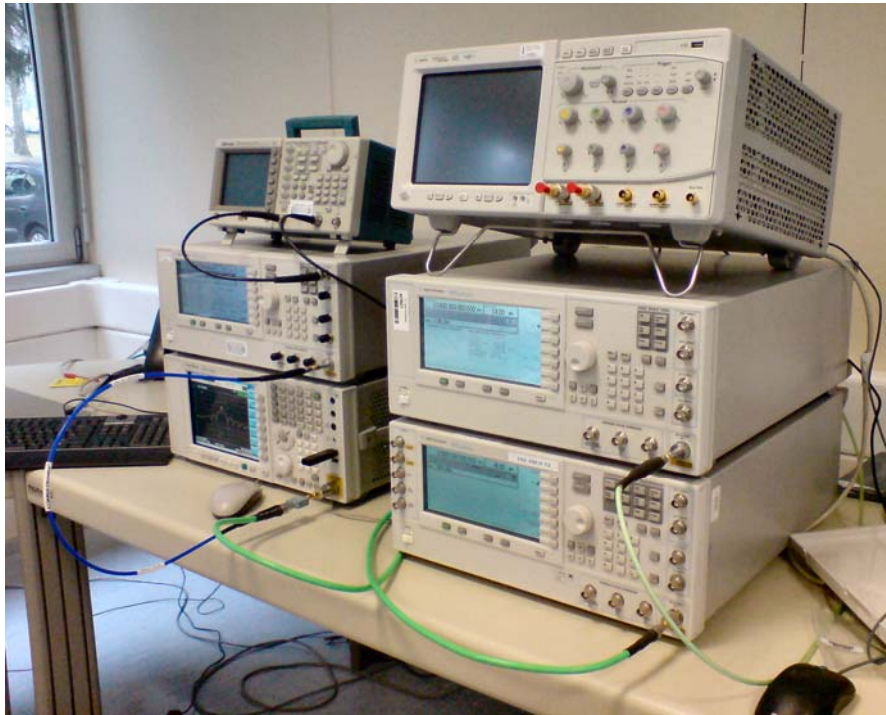


Figure 8: Victim and interfering signal generation

The 26 GHz victim signal was generated by means of an arbitrary waveform generator. Because the acquisition and analysis bandwidth of the Agilent signal analyser was limited to 40 MHz all measurements were made with a victim signal bandwidth of 28 MHz.

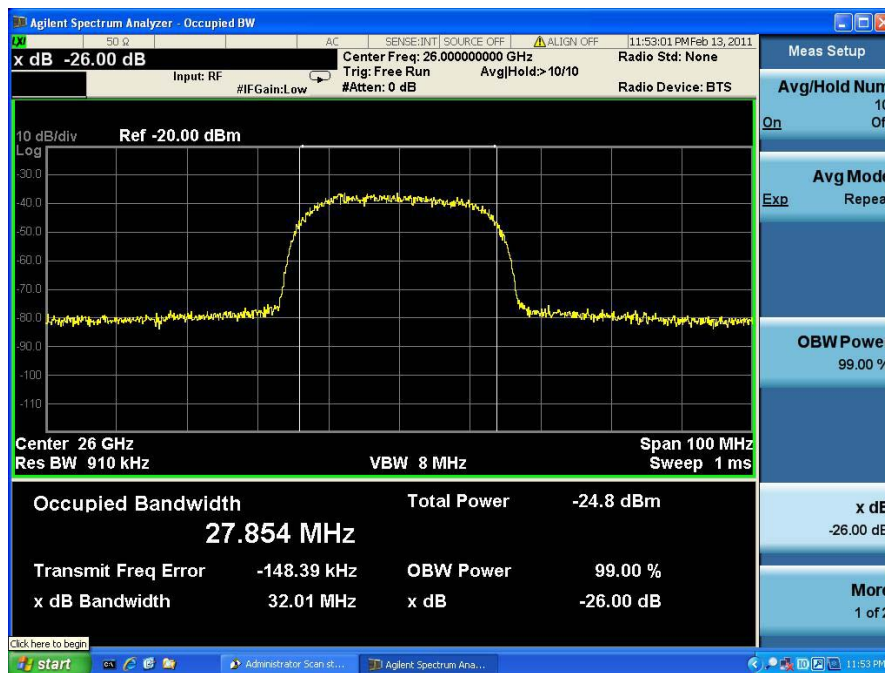


Figure 9: Victim signal (centre frequency: 26 GHz, channel bandwidth: 28 MHz)

Commercial FS PTP systems support a wide range of modulations. It would have been too time-consuming to test them all; therefore we focused on the higher-capacity modulations 64-QAM, 128-QAM, and 256-QAM in this study.

The first step was to optimise the signal path (and thus minimise the victim signal EVM) using the adaptive equaliser function of the spectrum analyser. In the second step the victim signal level was reduced to a level that resulted in a SNR corresponding to a BER¹ of 10⁻⁶.

BER	64QAM		128QAM		256QAM	
	SNR [dB]	EVM	SNR [dB]	EVM	SNR [dB]	EVM
10 ⁻³	22,6	7,4%	25,7	5,2%	28,4	3,8%
10 ⁻⁴	24,3	6,1%	27,4	4,3%	30,2	3,1%
10 ⁻⁵	25,5	5,3%	28,6	3,7%	31,6	2,6%
10 ⁻⁶	26,5	4,7%	29,5	3,4%	32,6	2,3%
10 ⁻⁷	27,4	4,2%	30,2	3,1%	33,4	2,1%
10 ⁻⁸	28,1	3,9%	30,8	2,9%	33,4	2,1%
10 ⁻⁹	28,6	3,7%	31,2	2,7%	34,7	1,8%

Table 4: BER and the corresponding SNR and EVM values for different modulations

Next, the interfering signal was added, starting at an I/N level of -32 dB. The output power level of the UWB signal generator had been adjusted for each pulse so that the maximum mean power level remained constant for all pulses. The signal level was then increased in steps of 2 dB and the impact on the average victim EVM was recorded. The correlation of the EVM and the interfering signal (indicated by the I/N ratio) for one of the investigated pulse types is shown in Figure 10. In order to make sure even the longest UWB burst (96 μs) was captured in its entirety the EVM was averaged over 2099 symbols which corresponds to approx. 100 μs. This procedure was repeated for a number of combinations of pulse type, victim modulations, and duty cycle.

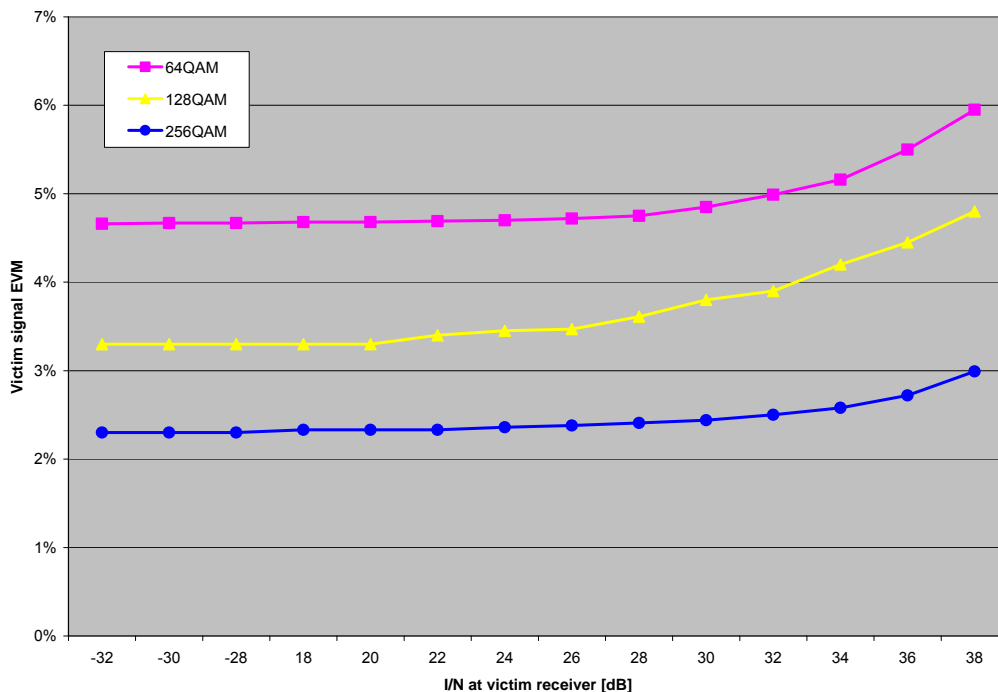


Figure 10: Victim signal EVM vs. SRR interference level for various victim signal modulation types (SRR pulse width=20 ns, PRI = 180 ns)

¹ See note on BER in section 2. Test concept

An exemplary spectrum analyser display is shown in Figure 11. Spectrum, EVM and the constellation of a 128-QAM signal are displayed.

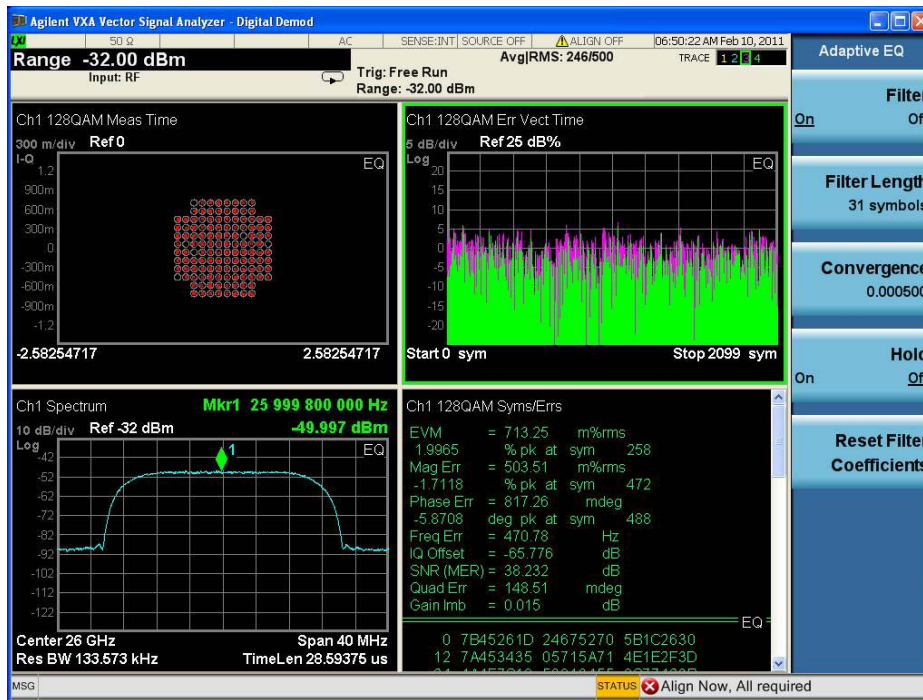


Figure 11: Victim signal (centre frequency: 26 GHz, modulation: 128-QAM), no interference

Figure 12 shows the spectrum of one of the UWB signals used in this study.

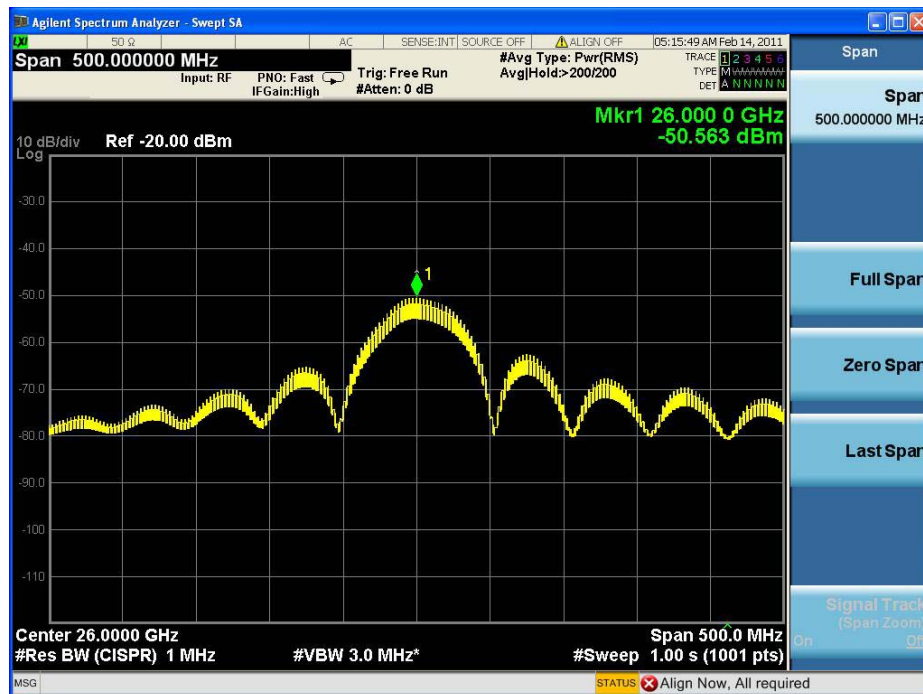


Figure 12: Spectrum of a pulse train (Pulse width = 20 ns, PRI = 800 ns)

5.2 Measurement results – Single-source interference

The first set of measurements was made with continuous UWB signals, i.e. with a duty cycle of 100%. The following observations were made:

- A measurable deterioration of the victim EVM occurred from SINR levels of 32 dB on, corresponding to an I/N ratio of 12 dB. At an I/N ratio of -20 dB which the ITU defined as minimum protection level for microwave fixed systems there was no measurable impact.
Note: Assuming two front SRR sensors per car, a UWB maximum mean transmit power spectral density of -50 dBm/MHz, a bumper loss of 3 dB, and a FS antenna gain of 40 dBi, an I/N ratio of 12 dB corresponds to a LOS distance between car and FS receiver of approx. 18 m.
- For pulses of identical mean power levels and pulse widths, the level of interference generally increased with the length of the pulse repetition interval. This indicates a relation between pulse peak power and the receiver's ability to demodulate the signal. The measurement results for the three modulation types are provided in Figure 13 - Figure 15.

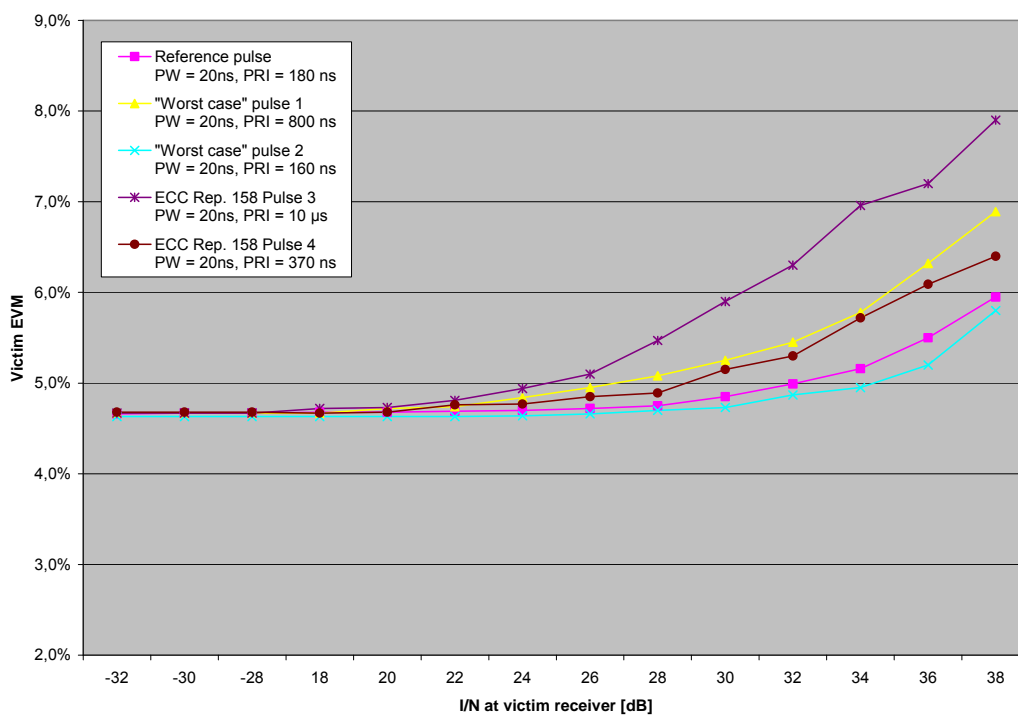


Figure 13: Victim signal EVM vs. SRR interference level for various SRR pulse types (victim signal modulation: 64-QAM)

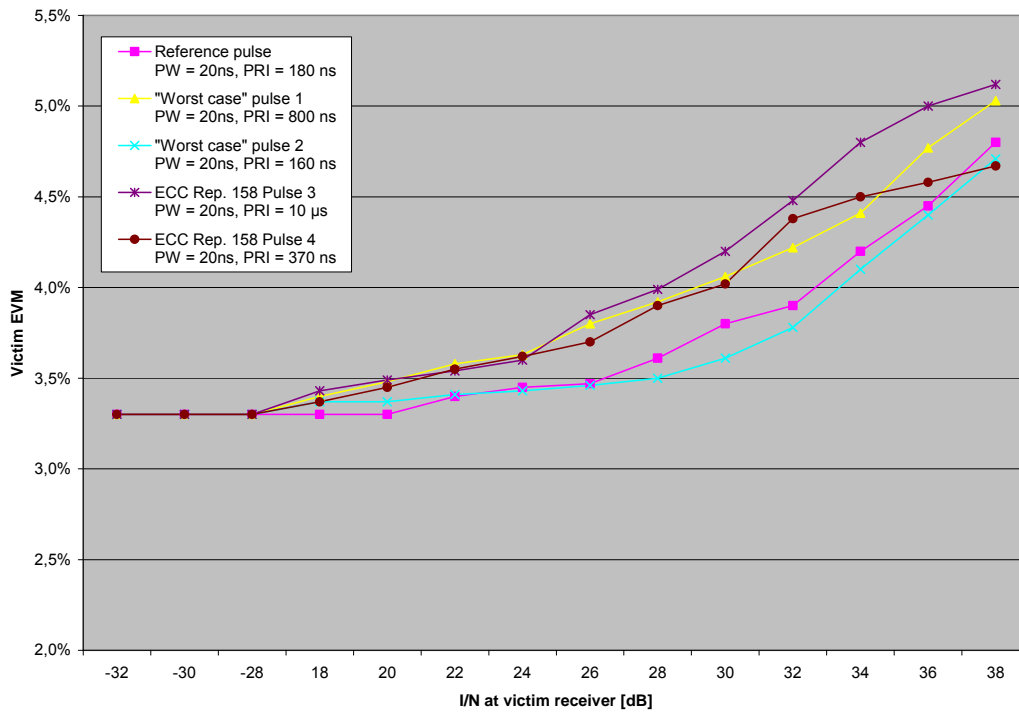


Figure 14: Victim signal EVM vs. SRR interference level for various SRR pulse types (victim signal modulation: 128-QAM)

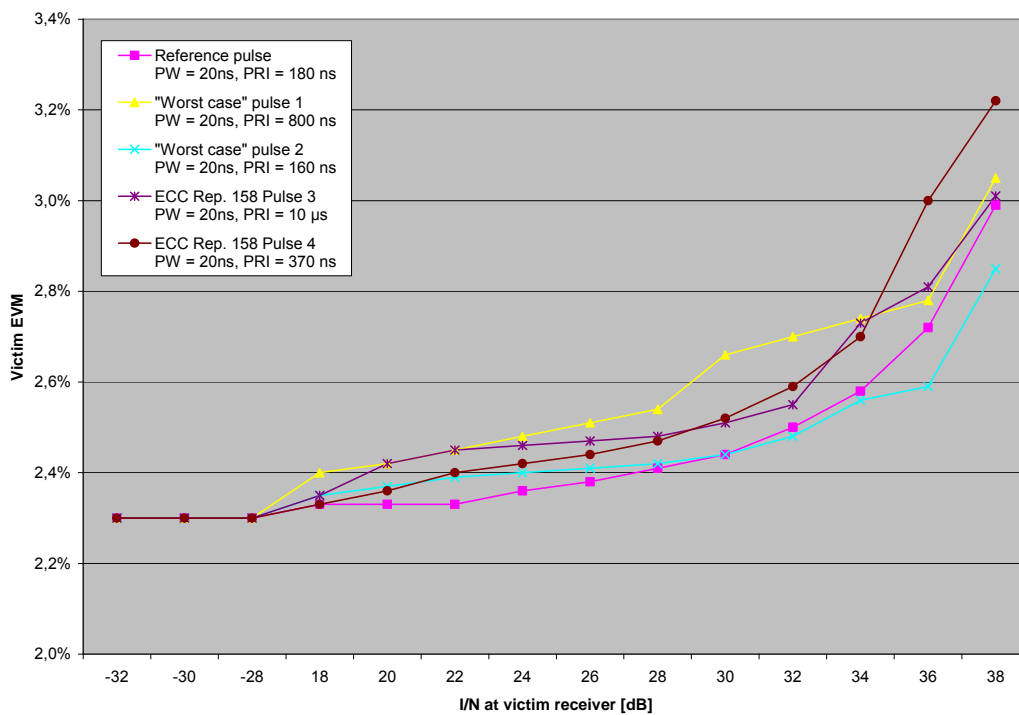


Figure 15: Victim signal EVM vs. SRR interference level for various SRR pulse types (victim signal modulation: 256-QAM)

In a second set of measurements duty cycles were applied to the UWB signals. We distinguished between two cases:

- Case 1: The UWB transmit power settings remained unchanged so that the application of duty cycles resulted in a reduction of the maximum mean power levels.
- Case 2: The UWB transmit power settings were adapted according to the duty cycle so that the maximum mean power level was constant for all pulses and identical to the continuous case.

As the first set of measurements had not indicated any fundamental difference between the different victim modulation types, we decided to restrict the measurements to the 128-QAM case. The following observations were made:

- Case 1: Measurable deterioration of the victim EVM occurred at significantly lower SINR levels as in the continuous case, with some variation depending on the pulse type. Interference was reduced in proportion to the duty cycle applied, i.e. for a DC of 10% the SINR improved by 10-12 dB, for a DC of 2% by 14-18 dB. Figure 16 shows the victim signal EVM vs. the interfering signal power for different pulse types with a duty cycle of 10%. Like in the continuous case, the level of interference increases with the PRI length.
- Case 2: Although the adaptation of the mean power according to the duty cycle corresponds to an increase of the peak power, interference was reduced by 4-8 dB compared to the continuous case. Figure 17 shows the victim signal EVM vs. the interfering signal power for different pulse types with a duty cycle of 10%. With the exception of Pulse no. 4 the correlation between interfering power and victim EVM follows the same rule as in the previous measurements. The reason for this deviation could not be identified.

Figure 18 compares the impact on the victim EVM for one type of UWB pulse with different duty cycles and power levels.

- For pulses of identical mean power level and duty cycle, the level of interference was slightly higher for pulses wider than the symbol duration of the victim signal (see Table 5). This observation which indicates a relation between the amount of overlap between interfering pulse and victim symbol and the impairment of the victim signal is in line with findings from a recent study on interference from LDC UWB to Mobile WiMAX.

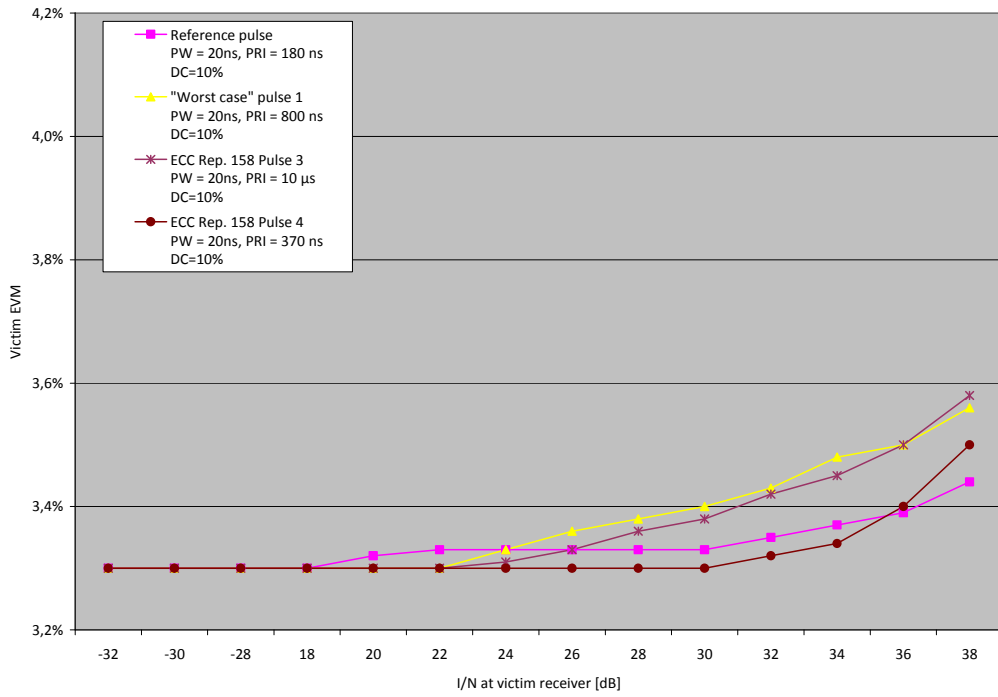


Figure 16: Victim signal EVM vs. SRR interference level for various SRR pulse types (duty cycle: 10%, constant peak power)

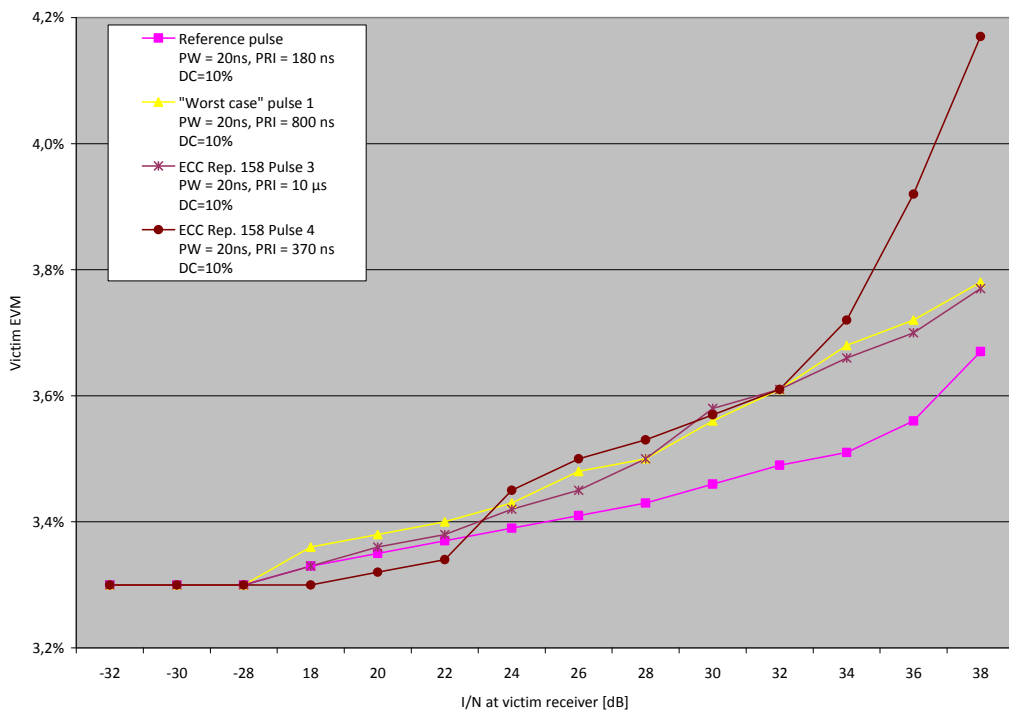


Figure 17: Victim signal EVM vs. SRR interference level for various SRR pulse types (duty cycle: 10%, constant mean power)

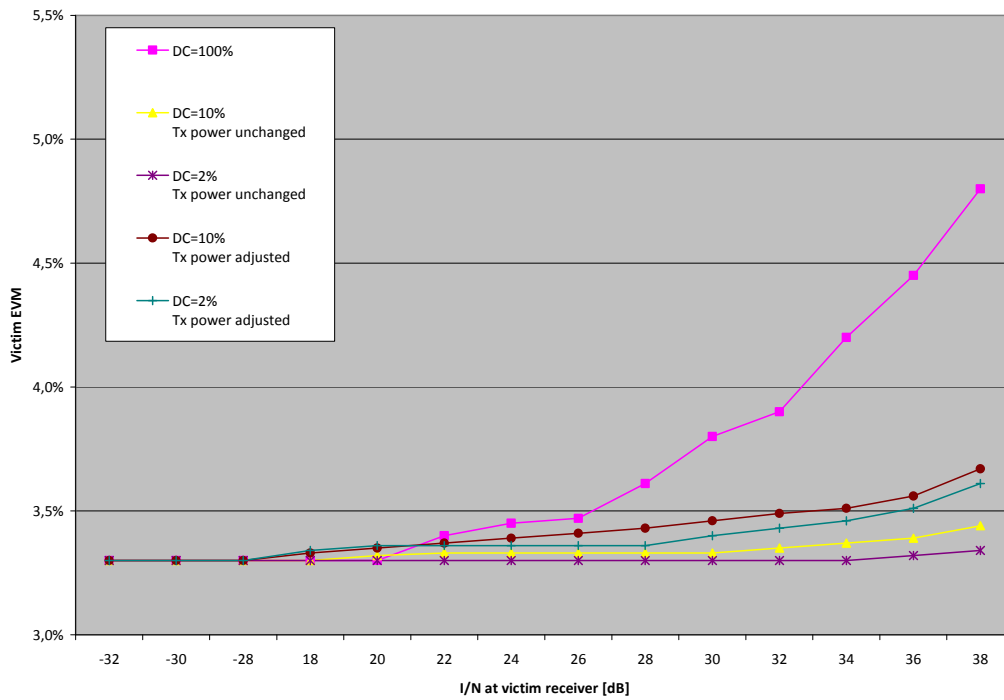


Figure 18: Victim signal EVM vs. SRR interference level for various SRR duty cycles (SRR pulse width=20 ns, PRI = 180 ns)

To generate a victim signal bandwidth of 28 MHz that complies with the limits of spectral power density for FS PTP systems specified in [7], the symbol rate was set to 21 MHz (filter roll-off factor of 0.35). This symbol rate corresponds to a symbol duration of 48 ns.

With the interfering signal switched off, the victim signal power was set to a level that resulted in an EVM of 3.4%. Then, interference from different UWB pulses of identical peak and mean power but different pulse widths was generated.

	No pulse	Pulse 1	Pulse 2	Pulse 3
Pulse width [ns]	-	20	50	100
PRI [ns]	-	180	450	900
PRF [MHz]	-	5,56	2,22	1,11
Duty cycle	-	11,1%	11,1%	11,1%
Victim EVM	3,4%	4,1%	4,2%	4,3%
Corresponding BER	10^{-6}	$<10^{-4}$	$<10^{-4}$	$<10^{-3}$

Table 5: Impact of pulse width on the victim EVM (128-QAM signal)

Interference from Pulse 1, with a width significantly smaller than the victim symbol duration, was lower than that of Pulses 2 and 3, which were wider than the victim symbol duration.

5.3 Measurement results - Aggregate interference

For quantifying the impact of LDC on the quality of victim signal the power of the aggregate interference signal was first set to a level that resulted in a victim EVM value corresponding to a BER of 10^{-4} . Then, different duty cycles were applied and the impact on the victim EVM was recorded. Owing to time limitations, we again restricted the scope of our measurements to the 128-QAM modulation.

Observations:

For all deployment scenarios the application of duty cycles reduced the level of interference albeit not to the same extent as in the single interferer cases. A DC of 10% resulted in a reduction of 3-6 dB; a DC of 2% yielded a reduction of 8-12 dB. In terms of BER a DC of 10% yields an improvement by one order of magnitude, from (10^{-4} to 10^{-5}), and a DC of 2% yields an improvement by two orders of magnitude, from (10^{-4} to 10^{-6}), when compared to a continuously transmitted UWB signal (BER= 10^{-4}). Figure 19 - Figure 21 illustrate the impact of LDC for different pulses and market penetration rates.

For UWB signals with DCs between 2% and 10% the variation of market penetration between 7% and 100% had only a minor impact on the EVM. This observation is in line with the results of our calculations of the contribution of each interferer (Figure 22 and Figure 23).

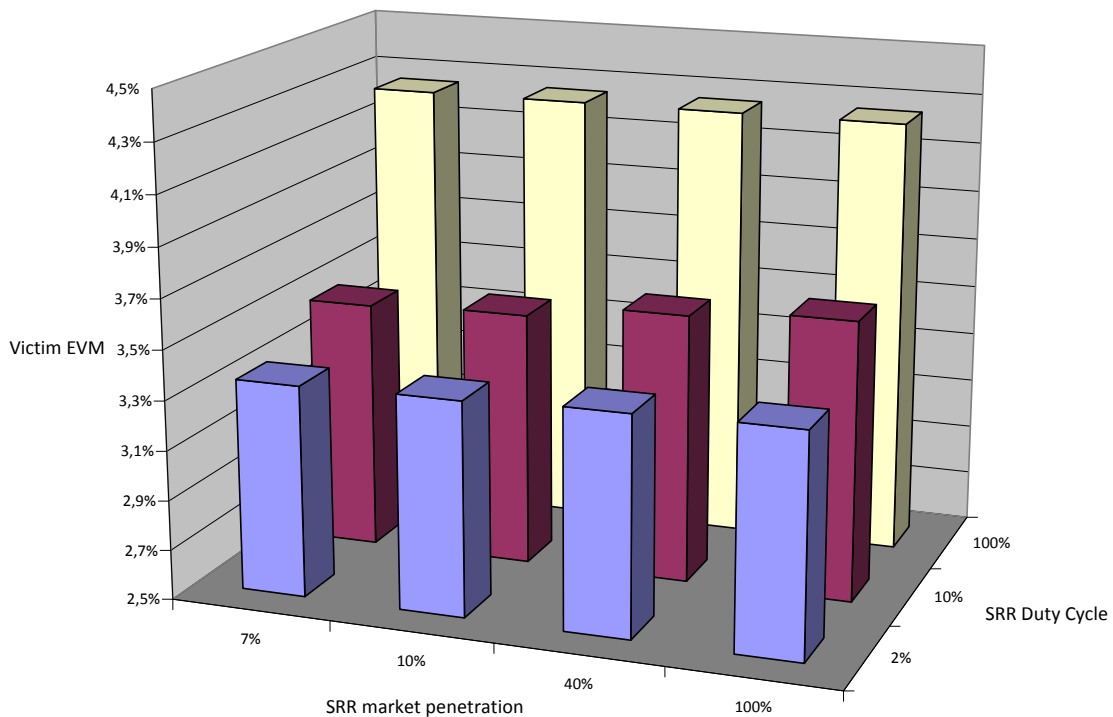


Figure 19: Reference pulse 1 (width 20 ns, PRI 180 ns)

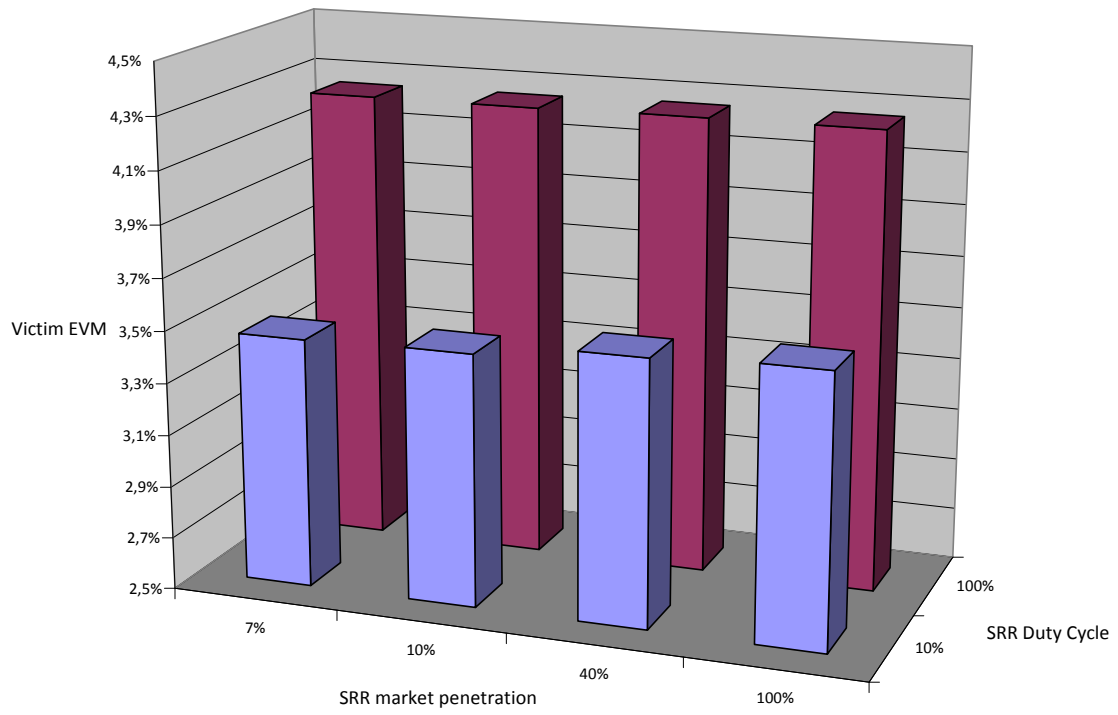


Figure 20: "Worst case" pulse 1 (width 20 ns, PRI 800 ns)

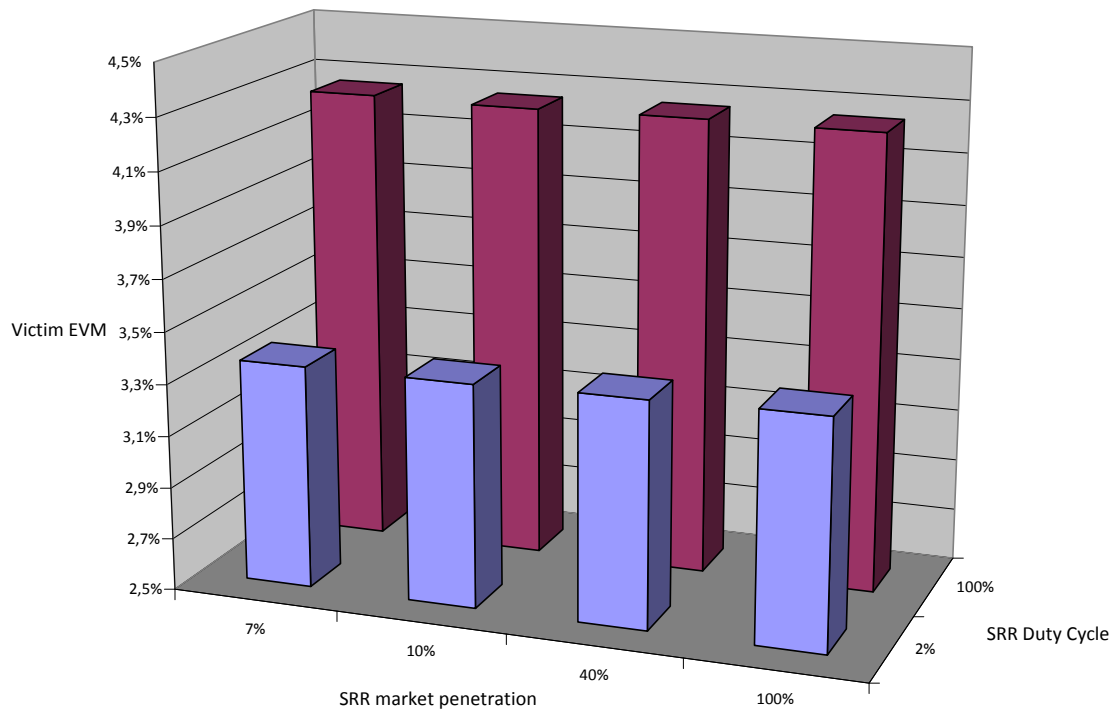


Figure 21: "Worst case" pulse 2 (width 20 ns, PRI 160 ns)

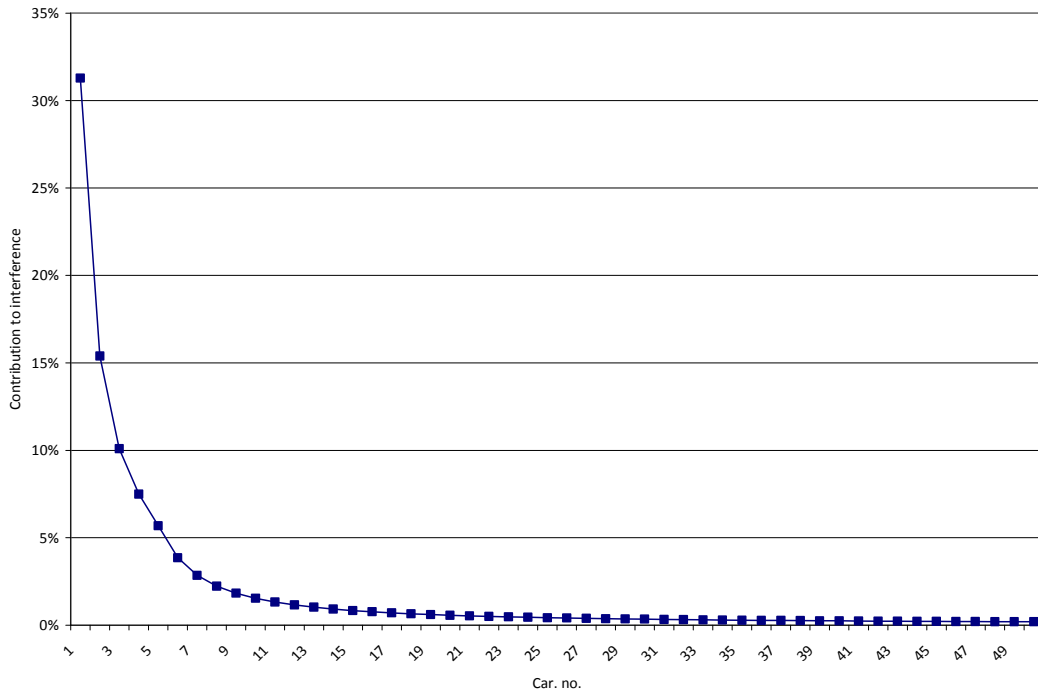


Figure 22: Contribution of each car to the aggregate interference signal at the FS receiver (SRR penetration: 40%)

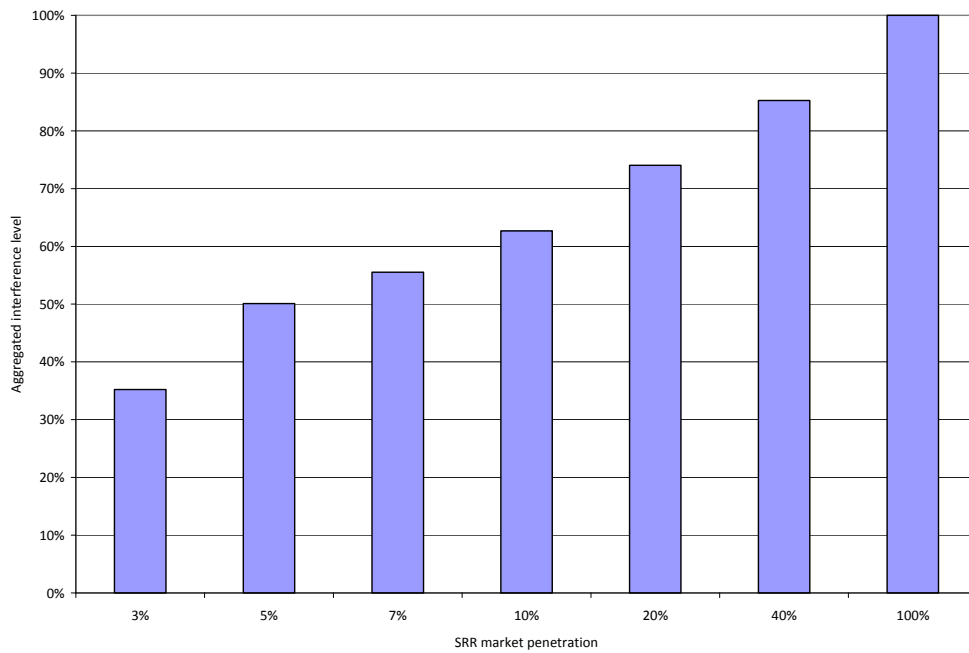


Figure 23: Aggregate interference levels vs. SRR market penetration (reference: SRR penetration=100%)

5.4 Simulation results – Summary

The simulation study was divided in two parts depending on whether a single interference node or multiple interferers are active. The presence of a single interference signal was initially considered in the analysis in order to evaluate the effects of the UWB signaling parameters, such as pulse width and PRI, on the evaluation metrics of the FS systems. Firstly, the simulation results showed that the pulse width duration of the individual UWB pulse has minimum impact on the BER and EVM of the FS systems if the same average power of the interference signal is maintained. Secondly, it was shown that the BER performances degrade considerably as the PRI increases for low noise-to-interference ratios. However, if $NIR = 20\text{dB}$ (maximum permissible interference level), the BER and EVM performances when $PRI = 180\text{ns}$ and $PRI = 800\text{ns}$ are almost identical for all the modulated FS systems.

Furthermore, the presence of aggregate interference was considered in the simulation analysis in order to evaluate the impact of the activity factor (AF), duty cycle and penetration factor (PF) on the evaluation metrics of the FS victim system. The simulation results showed that for all modulation schemes, the performance degradation remains low when DC increases but AF and PF are low. However, the BER and EVM performance degradation was significant when both AF and DC were 100%. It was concluded that the system performance degradation resulting from increasing the PF is lower than the one obtained by increasing the AF. Finally, it was found that, under the defined scenario conditions, if the average power of the interference nodes increases to $P_s = -41.3$ dBm/MHz, the BER and EVM performances degrade noticeably and it can only be combated if both AF and DC are significantly low.

The detailed simulation results are provided in Annex A.

6. Summary and Conclusion

A comprehensive study to evaluate the impact of LDC on the level of interference generated by automotive UWB SRR systems in the 24.25-26.65 GHz range was performed by means of measurements and simulations. The effects of single-source and aggregate interference on wireless fixed service links operating at 25 GHz and at 26 GHz were studied. Victim and interfering signals were generated by means of arbitrary waveform generators.

Two metrics, BER and EVM, were measured or computed at the FS victim receiver for a number of different modulation schemes including BPSK, QPSK, 16-QAM, 64-QAM and 128-QAM.

The conclusions that have been drawn from the study can be summarized as follows:

1. The measurements showed that introducing a duty cycle between 2% and 10% as proposed in CEPT Report 37 can decrease the amount of interference from SRR to a FS receiver by up to 6 dB for a DC of 10 % and up to 12 dB for a DC of 2%. These figures refer to aggregate interference, based on the single-car entry scenario described in section 4.2 Aggregate interference. In case of single-source interference the reductions were approx. 6 dB higher.
2. For pulses of identical width and average power, the level of interference, i. e. the BER or EVM, increased with PRI, indicating an adverse effect of the peak power levels on the victim receiver's ability to demodulate the signal.
3. The impact of pulse width on the level of interference was small but there are indications that pulses shorter than the victim's symbol duration cause less interference than those as wide as or wider than symbol duration.
4. For duty cycles between 2% and 10% the SRR market penetration was found to play only a minor role, i.e. when increasing the penetration from 7% to 100% the measured interference level increased only slightly. For continuous SRR signals (DC = 100%), however, the level of interference increased considerably for penetration rates above 10%.
5. The SRR activity factor was found to have a bigger impact on the level of interference than market penetration, particularly for duty cycles > 20%.
6. From the analysis of the measurement and simulation results, and considering the general acceptance of the technical principles of the current regulation on automotive SRR systems, we conclude that **a modification of this regulation that applies the duty cycles and reduced SRR transmit power levels proposed in CEPT Report 37 should provide adequate protection for fixed services in the revised 26 GHz band.**

It is acknowledged that ideally an assessment of the interference impact on different services such as data, VoIP and video should have been performed on a commercial PTP system in order to complement the findings of the physical layer measurements. Such system, however, could not be obtained within the time frame available for this study. Due to the proprietary nature of PTP microwave systems, however, findings of such study might have been of limited value and probably not sufficient for formulating a generic statement on RF compatibility.

Annex A – Simulation report

The main objective of the simulation study is to model a realistic scenario in order to evaluate the interference effects, caused by the presence of multiple UWB SRR devices, on a Fixed Service radio link. In addition, the study aims to validate the measurements obtained in the conducted modality, presented above.

Several interference scenarios are considered in this work based on the selection of the pulsed UWB radar parameters, such as duty cycle (DC), penetration factor (PF), activity factor (AF), UWB pulse width and pulse repetition interval (PRI). The FS radio link is implemented by using four modulation schemes: binary phase-shift keying (BPSK), quadrature phase-shift keying (QPSK) and M-ary quadrature amplitude modulation with modulation orders $M = 16$ and $M = 64$.

The system performance is evaluated through the analysis of the estimated bit error rate and error vector magnitude metrics under different types of interference sources.

A.1 Evaluation Metrics

Two metrics are considered to evaluate the FS system performance. The first metric, the estimated average BER, is the ratio between the number of erroneous bits received and the total number of transmitted bits. The BER is commonly expressed as a function of the E_b/N_0 , which is the ratio between the energy per bit (E_b) and the noise spectral density (N_0). Also, the BER can be expressed as a function of the transmitted signal-to-noise ratio $SNR_{Tx} = P_s/P_n$, where P_s is the total transmitted power and P_n is the noise power. SNR_{Tx} and the E_b/N_0 are related as follows:

$$SNR_{Tx} = E_b/N_0 + 10\log_{10}(n) + 10\log_{10}\left(\frac{R_s}{BW}\right), \quad (1)$$

where SNR_{Tx} and E_b/N_0 are expressed in dB units, $n = \log_2(M)$ is the number of bits per symbol, R_s is the symbol rate and BW is the signal bandwidth.

In this work, the average BER metric is computed as a function of the received signal-to-noise ratio, $SNR = P_r/P_n$, where P_r is the power of the victim signal measured at the input of the received antenna. The relationship between P_r and P_s is given by the Friis transmission equation as

$$P_r = \frac{P_s G_t G_r}{L_p}, \quad (2)$$

where G_t and G_r are the transmitter and receiver antenna gains respectively, and L_p models the propagation losses.

The other metric employed in this study is the EVM. The EVM, also called the receive constellation error, accounts for the error distance between the received constellation data point and its ideal value in the case of high signal-to-noise ratio and interference-free situations. Both metrics, SNR and EVM, provide the same information since they are inversely proportional. The advantage of using

EVM with respect to the BER is that EVM is a faster parameter to estimate, since it is measured at the input of the symbol decision block in the receiver chain. The EVM values are calculated from

$$EVM = \frac{\frac{1}{N_{sym}} \sum_{m=1}^{N_{sym}} |r_{op}[m] - r_i[m]|^2}{\frac{1}{N} \sum_{m=1}^N |r_{op}[m]|^2}, \quad (3)$$

where N_{sym} is the total number of transmitted symbols and $r_{op}[m]$ and $r_i[m]$ are the i -th optimum and received constellation points respectively.

A.2 System Model

The high level block diagram of the simulation model is represented in Figure 24. The radiated transmitted signal of the victim FS system is a single-carrier signal whose mathematical expression is given by [12] :

$$s(t) = \sum_{m=1}^{N_{sym}^F} \left(A_m^i \sqrt{\frac{E_g}{2}} \phi_1(t - mT_s^F) + A_m^q \sqrt{\frac{E_g}{2}} \phi_2(t - mT_s^F) \right), \quad (4)$$

where N_{sym}^F is the total number of transmitted symbols. Furthermore, the signals $\phi_1(t)$ and $\phi_2(t)$ are the basis functions, are given by

$$\phi_1(t) = \sqrt{\frac{2}{E_g}} g(t) \cos(2\pi f_c t); \quad \phi_2(t) = -\sqrt{\frac{2}{E_g}} g(t) \sin(2\pi f_c t). \quad (5)$$

The function $g(t)$ in (5) is modeled as a rectangular pulse of duration equal to a symbol time, $T_s^F = 1/R_s$, and energy value of E_g . The victim service is radiated at $f_c = 25$ GHz. Finally, the values of the quadrature and in-phase components, A_m^i and A_m^q , are determined according to the chosen modulation scheme as

$$\begin{aligned} A_m^i &= \pm 1; \quad A_m^q = 0; && \text{if BPSK} \\ A_m^i &= A_m^q = \pm 1; && \text{if QPSK} \\ A_m^i &= A_m^q = 2m - 1 - M; \quad \forall m \in \{1, 2, \dots, M\}; && \text{if M-QAM} \end{aligned} \quad (6)$$

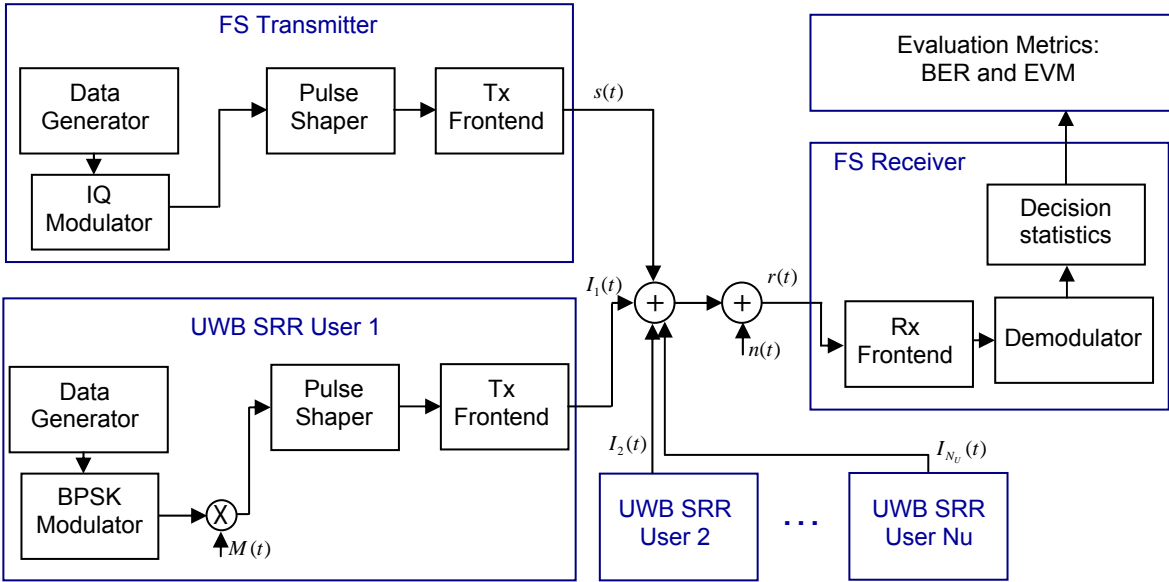


Figure 24: High-level block diagram of the simulation system

Note that the transmitter frontend blocks in Figure 24 include the digital-to-analog conversion (DAC) process, the mixer for up-converting the baseband signal to f_c and the transmitter antenna. A PSD realization of the FS transmitted signal is plotted in Figure 25.

The UWB SRR interference signal implemented in this work follows the pulsed frequency hopping (FH) version [6] [1]. The aggregate interference signal measured at the input of the victim FS receiver is composed of the sum of N_U active UWB SRR users. The analytical expression for the n -th UWB transmitted signal is expressed as

$$I_n(t) = \frac{1}{\sqrt{E_s^U}} \sum_{l=1}^{N_{sym}^U} \beta_l w(t) \cos(2\pi f_l t) \otimes M(t - lT_s^U - T_{asyn}^n), \quad (7)$$

where \otimes represents the convolution operator, N_{sym}^U is the number of UWB transmitted symbols, T_{sym}^U is the symbol duration, E_s^U is the energy of the UWB symbol and T_{asyn}^n is the asynchronous transmission time of the n -th UWB transmitter, which is uniformly distributed in $[0, T_{sym}^U)$. The basis pulse waveform, $w(t)$, of duration T_w is commonly implemented in UWB communications as a high order derivative of the Gaussian pulse in order to meet the restrictive power spectral masks imposed by the regulatory bodies [1] [6]. In this work, a simpler rectangular pulse of unitary energy is employed. The UWB SRR baseband signal is up-converted to a high frequency equal to $f_l = f_U + \lfloor l/N_p \rfloor BW_U$, where $f_U = 24.25 + BW_U [GHz]/2$ in GHz units, $BW_U \approx 2/T_w$ is the bandwidth of the UWB basic pulse waveform, N_p is the number of basic pulses per burst and $\lfloor \cdot \rfloor$ represents the floor function.

Finally, the signal $M(t)$ in (7) is written as

$$M(t) = \sum_{q=1}^{N_{burst}} \sum_{v=1}^{N_p} \delta_D(t - qT_{burst} - vT_p), \quad (8)$$

where $\delta_D(t)$ is the Dirac delta function. The parameters N_{burst} , T_{burst} and T_p are the number of bursts per symbol, the burst duration and the pulse repetition interval (PRI) respectively.

The received signal at the input of the FS receiver antenna in Figure1 is expressed as

$$r(t) = A^F s(t) + \sum_{n=1}^{N_U} A_n^U I_n(t) + n(t), \quad (9)$$

where A^F and A_n^U are the amplitude propagation losses of the victim FS signal and the n -th UWB SRR interferer respectively. The signal $n(t)$ in (9) is the additive white Gaussian noise (AWGN) contribution with double sided power spectral density (PSD) of $N_0/2$. At the FS receiver, the signal $r(t)$ goes through the receiver frontend block, which includes the following elements: a receiver antenna, a band-pass filter, a mixer for down-conversion and an analog-to-digital converter (ADC). Subsequently, the output signal of the receiver frontend is demodulated allowing the average BER and EVM to be computed.

A PSD realization of a filtered UWB SRR interference signal is plotted in Figure 25. An UWB signal with PRI $T_p = 180$ ns that uses rectangular pulse waveforms of duration $T_w = 40$ ns is generated in this example. The spectral lines are equally spaced by $1/T_p$ Hz.

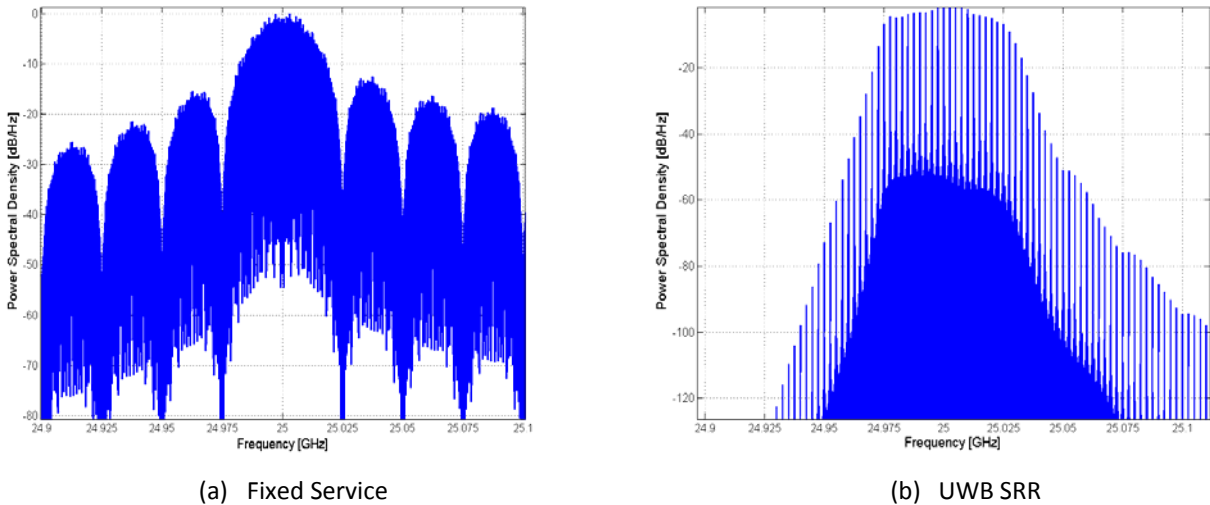


Figure 25: Normalized PSD realizations of the FS transmitted signal and a single filtered UWB SRR interference signal.

A.3 Simulation Analysis

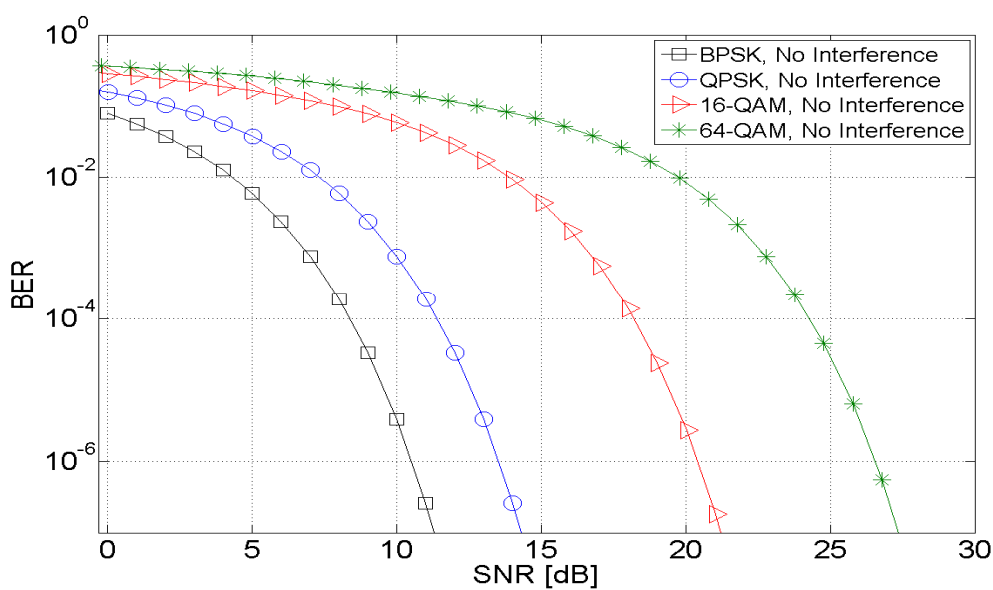
The simulation study is divided in two parts depending on whether a single interference node or multiple interferers are present. Initially, a single UWB SRR sensor is considered in the analysis in order to evaluate the effects of the UWB signaling parameters, such as pulse width and PRI, on the BER and EVM performances of a FS radio link. Subsequently, an aggregated interference signal is implemented based on the scenario depicted in Figure 6. In this interference context, the selection of three UWB SRR system parameters, such as the duty cycle (DC), activity factor (AF) and penetration factor (PF), is thoroughly evaluated in this section. These parameters are defined as $DC = T_{burst} / T_{sym}^U$, $AF = N_{sa} / N_{sc}$ and $PF = N_{ca} / N_{cars}$, where N_{sa} , N_{sc} , N_{ca} and N_{cars} are the number of active sensors per car, the number of available sensors per car, the number of active cars with UWB capabilities on the road and the maximum number of cars equipped with UWB SRR devices. In this work, $N_{sc} = 2$ and $N_{cars} = 125$ are considered as described in section X.

A.3.1 Single Interferer

At the outset, the BER and EVM performances as a function of the received SNR are plotted in Figure 3 considering the AWGN to be the only impairment. The receiver sensitivity is related to the minimum received SNR value that guarantees a BER value of 10^{-6} . Under these conditions, the received SNR values that provide a BER = 10^{-6} , named here SNR_R , for each modulated FS system can be measured from Figure 26 and are summarized in Table 6.

Modulation	BER	SNR_R [dB]	EVM [%]
BPSK	10^{-6}	10.50	30.00
QPSK	10^{-6}	13.50	21.24
16-QAM	10^{-6}	20.40	9.60
64-QAM	10^{-6}	26.55	4.73

Table 6: SNR and Percentage EVM for BER values of 10^{-6}



(a) BER vs. SNR

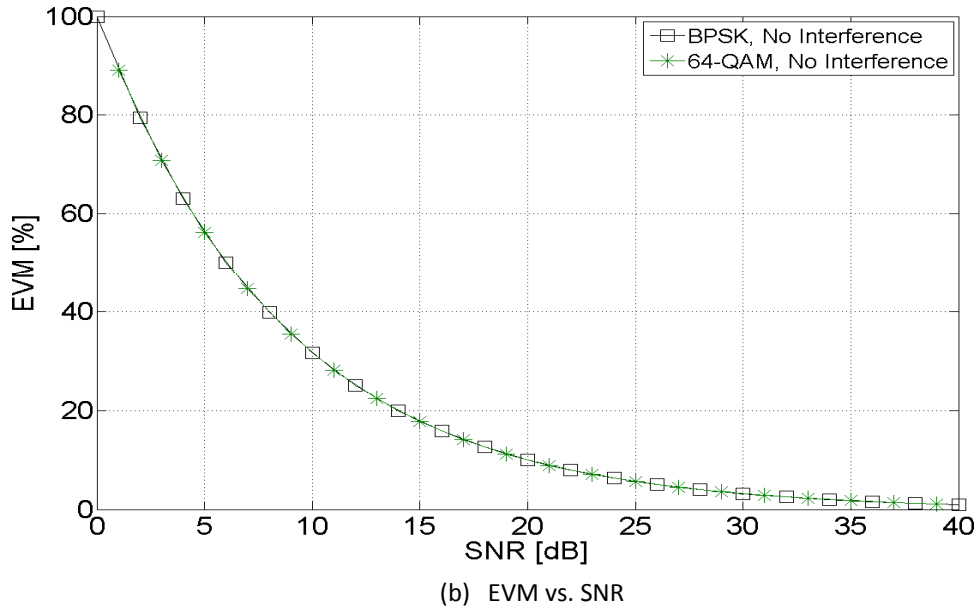


Figure 26: BER and percentage EVM as a function of the received SNR values (without interference)

In the following scenario, the presence of a single interference signal with DC=100%, and AF=100% is considered. The objective of this simulation work is to evaluate the interference impact on the BER and EVM performances of the different modulated FS systems, caused by the intrinsic properties of the UWB pulses (i.e. pulse repetition interval and pulse width). The simulation results are plotted in Figure 27 - Figure 30 for BPSK, QPSK, 16-QAM and 64-QAM modulated FS systems respectively. The evaluation metrics, BER and percentage EVM, are computed as a function of the noise-to-interference ratio (NIR) measured at the input of the receiver. In this simulation scenario the SNR value is fixed to SNR_R , the values of which are provided in Table 6 for each modulation scheme.

The BER performances for a BPSK system in the presence of an UWB interference signal with different pulse widths and fixed $PRI = 800\text{ns}$ are illustrated in Figure 4. The simulation results show that changing the UWB pulse width value while maintaining the same average power has minimum impact on the BER since all the energy of the interfering signal goes through the FS receiver filter of 50 MHz bandwidth. Subsequently, three simulations were performed with UWB SRR interference signals (using $T_w = 40\text{ns}$) having PRI values of 180ns, 800ns and $10\mu\text{s}$ respectively. The simulation results, presented in Figure 27 - Figure 30, show that the BER performances degrade considerably as the PRI increases. As an example of this, in the case of $NIR = 10\text{dB}$, BER values of 6×10^{-6} , 4×10^{-5} and 2×10^{-3} are obtained for $PRI = 180\text{ns}$, $PRI = 800\text{ns}$ and $PRI = 10\mu\text{s}$ respectively. Nevertheless, when the $NIR = 20\text{dB}$ (maximum permissible interference level), the BER and EVM performances when $PRI = 180\text{ns}$ and $PRI = 800\text{ns}$ are almost identical for all the modulated FS systems. Therefore, $PRI = 800\text{ns}$ and $T_w = 40\text{ns}$ are the chosen values for the following interference scenarios.

A.3.2 Aggregate Interference Effects

The initial reference scenario is depicted in Figure 6, where a maximum number of 125 cars, each one equipped with 2 UWB SRR sensors, are present in a 3 km range. In this interference context, the location of the closest car to the FS receiver is determined in order to comply with the maximum

allowed transmitted power requirements [1]. Thus, the distance of the nearest UWB SRR sensor with respect to the mast of the FS receiver is set to $d_1 = 12\text{m}$, which gives a $d_{ant} = \sqrt{d_1^2 + (h_R - h_s)^2} = 15.3\text{m}$, where d_{ant} is the line of sight distance between UWB SRR sensor and FS receiver antenna. Furthermore, the noise power measured in a 50MHz bandwidth is approximately -97dBm and the propagation losses based on the free-space path loss model is 84 dB when $f_c = 25\text{GHz}$. Taking into consideration that the transmitted average power of the UWB SRR node is -50dBm/MHz, a required protection level of $\text{NIR} = 20\text{dB}$ is fulfilled in this scenario. In this analysis, both transmitter and receiver antennas are omnidirectional types with 0 dBi gain.

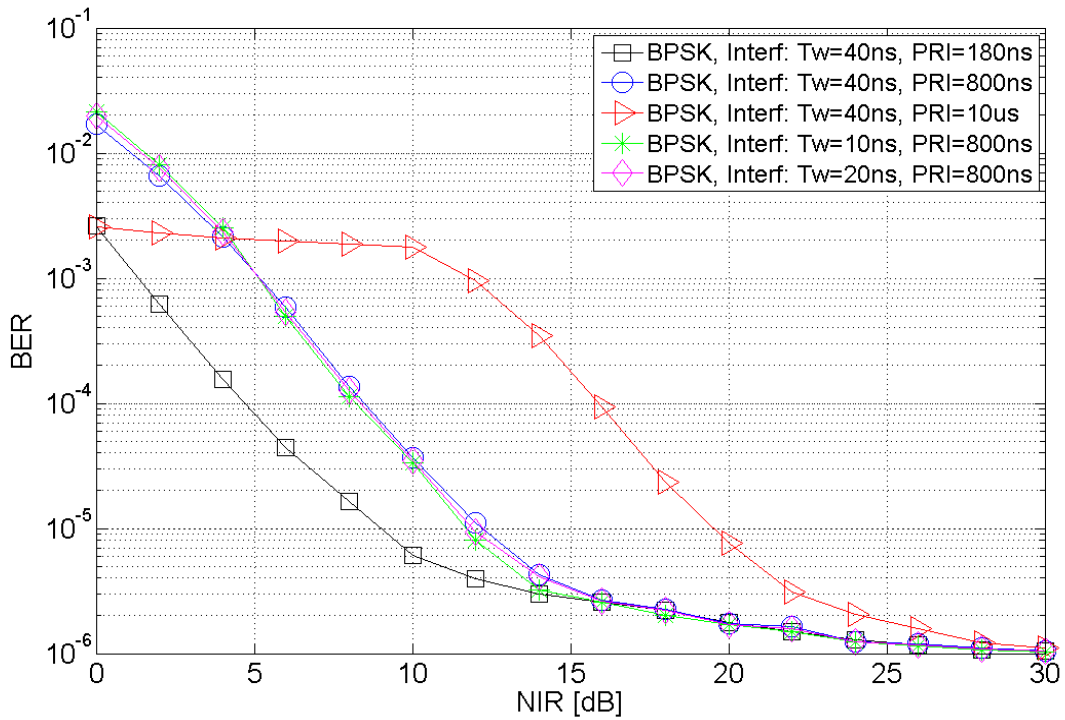
Firstly, the effect of the DC on the BER and EVM metrics of the FS systems are plotted in Figure 31-Figure 34 for BPSK, QPSK, 16-QAM and 64-QAM modulation schemes respectively. In this simulation scenario, two different AF values are considered, $\text{AF} = 50\%$ which implies one sensor per car is active and $\text{AF} = 100\%$ representing full activity of the cars present. Furthermore, four different PF values are considered in the simulations in order to model the aggregate interference effects from low congested ($\text{PF} = 7\%$) to high congested roads ($\text{PF} = 100\%$). The active cars are sequentially displayed starting from the closest car to the FS victim receiver in order to account for the worst case interference scenario. In addition, the SNR values in this simulated scenario correspond to those ones defined in Table 6 for SNR_R . Also, the DC values change while maintaining the same peak power of the UWB interfering signal. The simulation results show that for all modulation schemes, the performance degradation remains low when DC increases but AF and PF are low. However, the BER of a BPSK modulated system in the presence of UWB SRR interference with $\text{DC} = 100\%$ degrades considerably from a value of 4×10^{-6} when $\text{AF} = 50\%$ to a value of 1×10^{-4} when $\text{AF} = 100\%$, even though the PF remains the same ($\text{PF} = 7\%$). In contrast, the BER performance degradation resulting from increasing the PF is lower than the one obtained by increasing the AF. This is reflected in Figure 30, where a BER value of 4×10^{-6} is measured when $\text{PF} = 7\%$ and $\text{BER} = 10^{-5}$ for $\text{PF} = 100\%$ (both interference signals employ $\text{AF} = 50\%$). The same behavior is manifested for each modulation scheme as illustrated in Figure 32-Figure 34.

Furthermore, the BER performances as a function of the received SNR are represented in Figures 12, 13, 14 and 15 for BPSK, QPSK, 16-QAM and 64-QAM modulated systems respectively. In this interference scenario, the penetration factor is fixed to $\text{PF} = 7\%$. The simulation results illustrate that the performance degradation of all the FS systems is large, as previously stated, when $\text{DC} = 100\%$ and $\text{AF} = 100\%$. In this situation, we find a $\text{BER} \approx 6 \times 10^{-5}$ when $\text{SNR} = \text{SNR}_R$. Nevertheless, the interference impact is noticeably reduced by decreasing the DC value, obtaining a $\text{BER} \approx 1.5 \times 10^{-6}$ for $\text{DC} = 10\%$ and $\text{AF} = 100\%$.

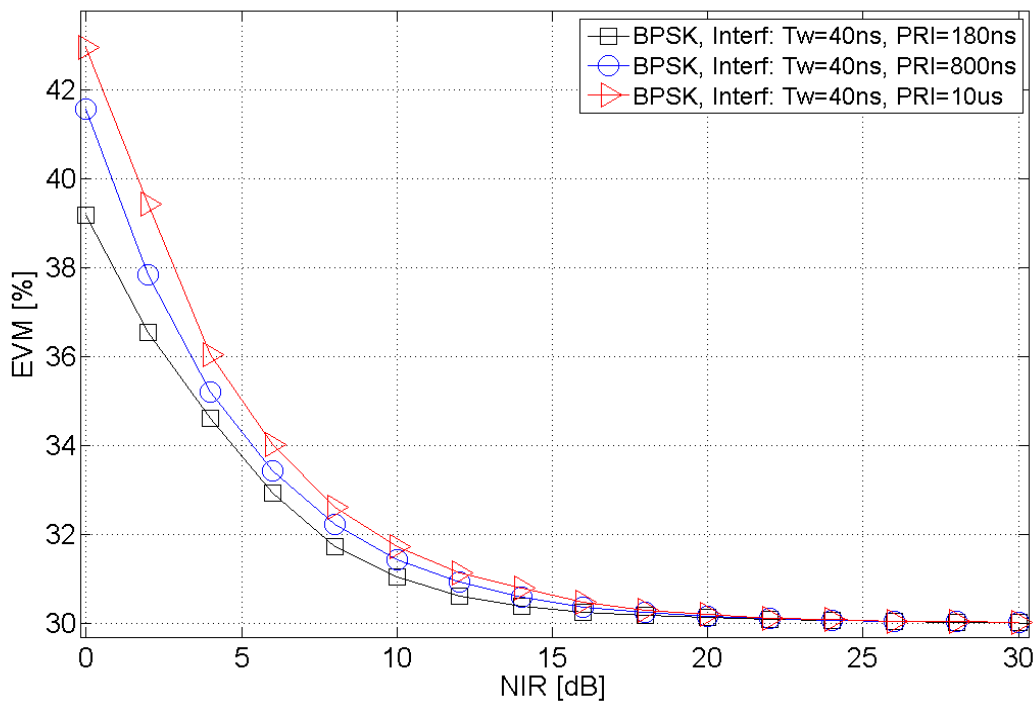
Subsequently, the effects of the PF on the BER and EVM performances of the four modulated FS systems are displayed in Figure 39-Figure 42 when the interference signals have an $\text{AF} = 100\%$ and the SNR is fixed to SNR_R . The simulation results show that the BER performance degradation caused by the increase of the PF is only significant when the DC is large. However, as previously indicated, the degradation caused by increasing the number of active cars from $\text{PF} = 7\%$ to $\text{PF} = 100\%$ is relatively low. This can be measured in Figure 39, where the EVM values are approximately 31.7% and 34.2% for $\text{PF} = 7\%$ and $\text{PF} = 100\%$ respectively, which corresponds to a relative degradation of 8% (2.5 % of the absolute EVM value). The same results are obtained for all the modulation schemes.

Finally, the BER and EVM performances as a function of the received SNR for both BPSK and 64-QAM modulated FS systems are plotted in Figure 43 and Figure 44 when an aggregate interference signal

of average power $P_s = -41.3$ dBm/MHz (the value assigned when $DC = 100\%$) is present. In this simulation scenario, $PF = 7\%$ and $AF = 100\%$ are considered. In this situation, the $NIR = 20$ dB, which was assigned to the UWB SRR node of the first car is not respected anymore. This results in a large degradation of the system performance when the SNR is large (the interference is the dominating impairment source) even in the situation of low duty cycle ($DC = 10\%$). In these conditions, a reduction of the AF and the use of very low DC values must be considered.

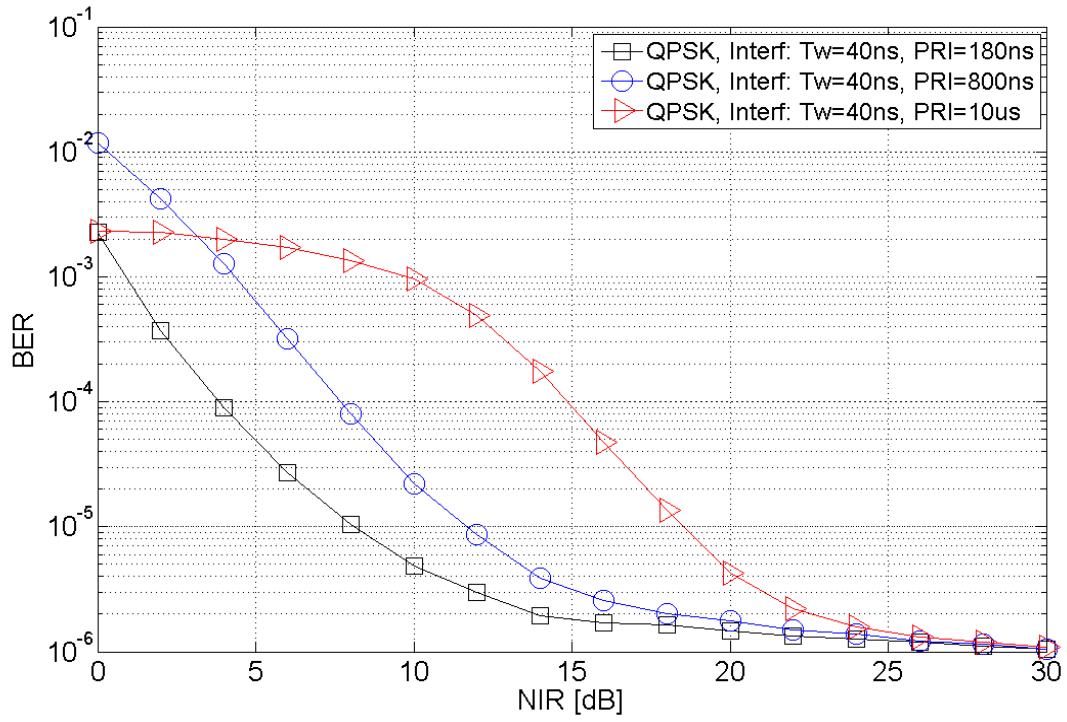


(a) BER vs. NIR

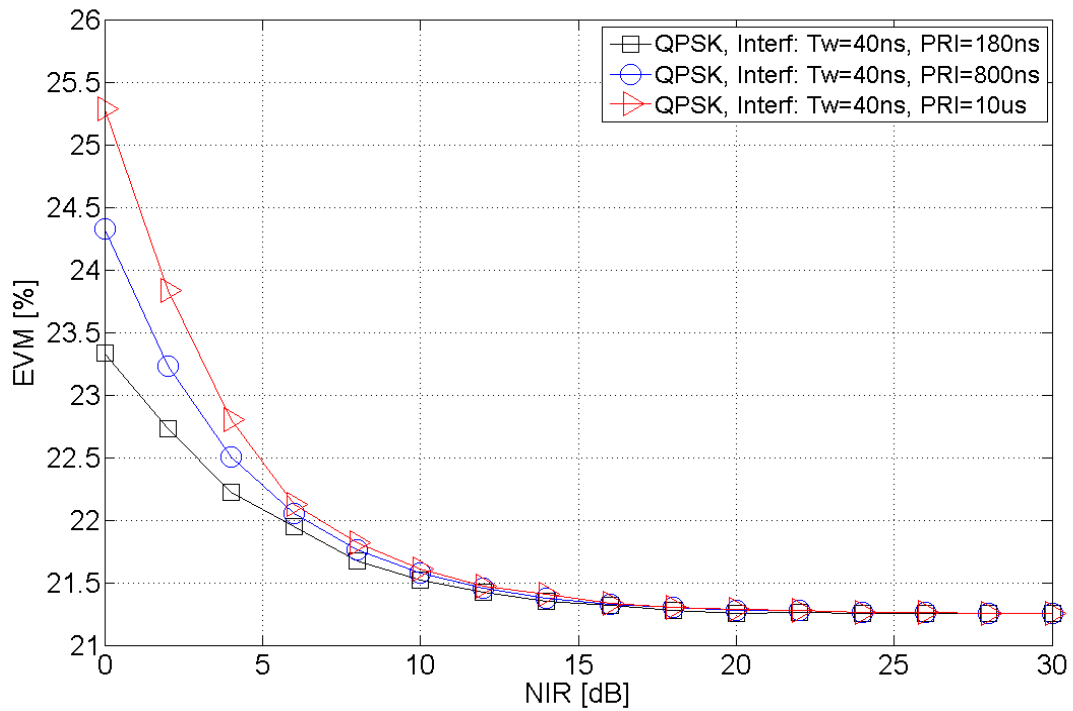


(b) EVM vs. NIR

Figure 27: BER and percentage EVM performances as a function of the NIR of a BPSK modulated FS system in the presence of a single UWB SRR interference with AF=100%, DC=100% and SNR = SNR_r.

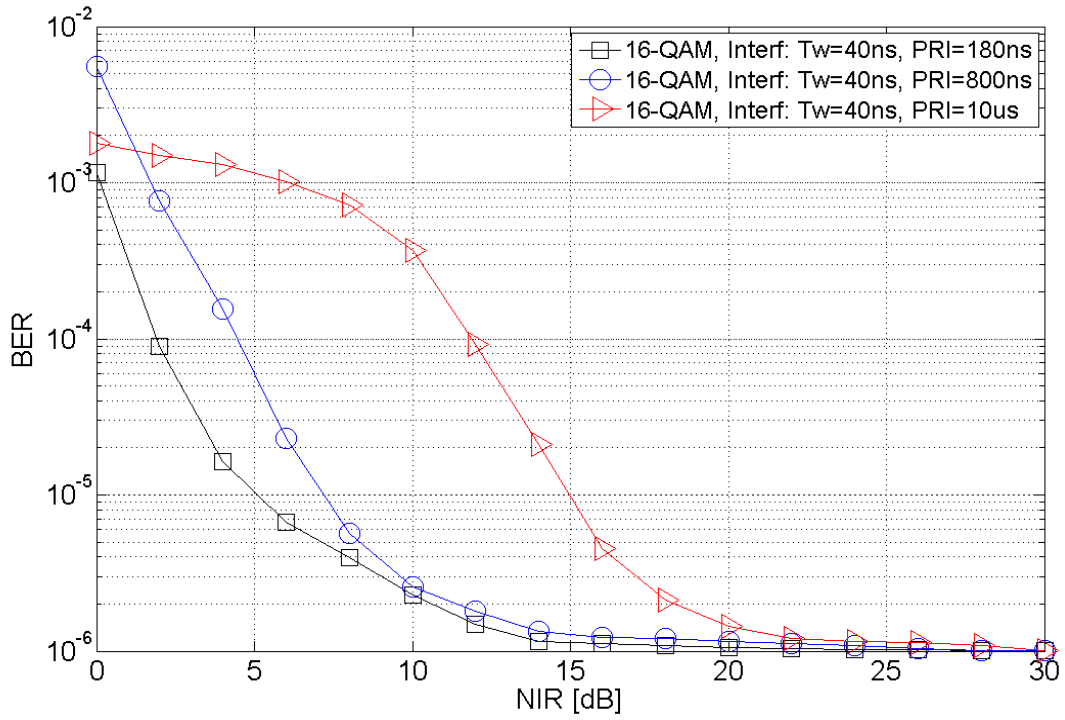


(a) BER vs. NIR

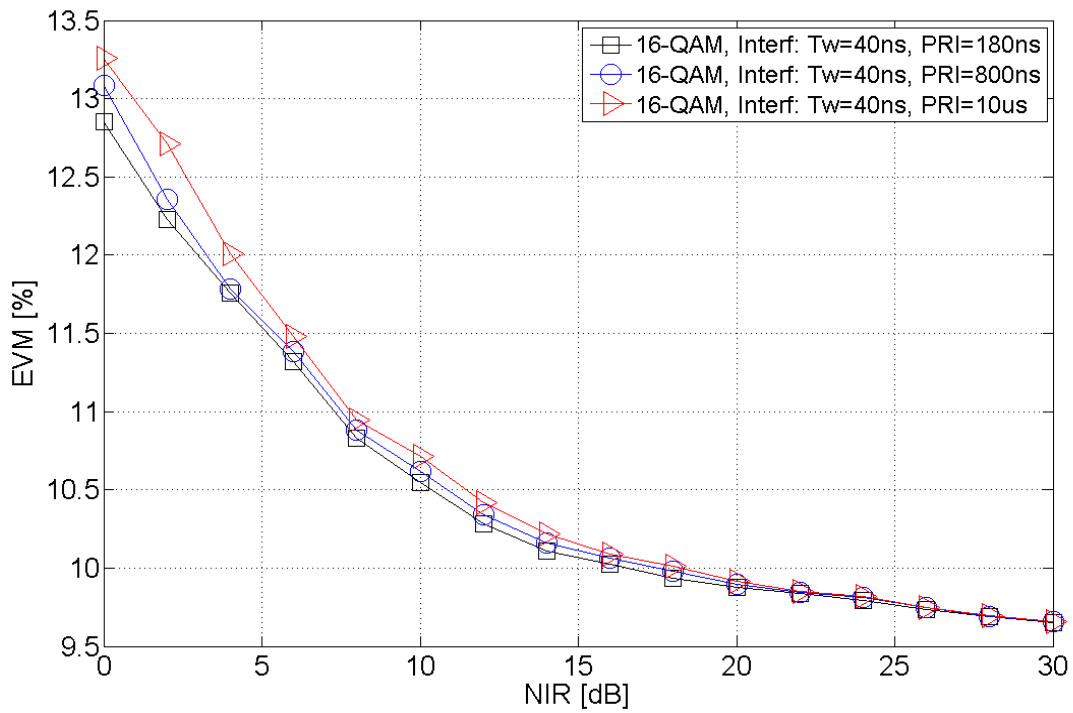


(b) BER vs. EVM

Figure 28: BER and percentage EVM performances as a function of the NIR of a QPSK modulated FS system in the presence of a single UWB SRR interference with $\text{AF}=100\%$, $\text{DC}=100\%$ and $\text{SNR} = \text{SNR}_R$.

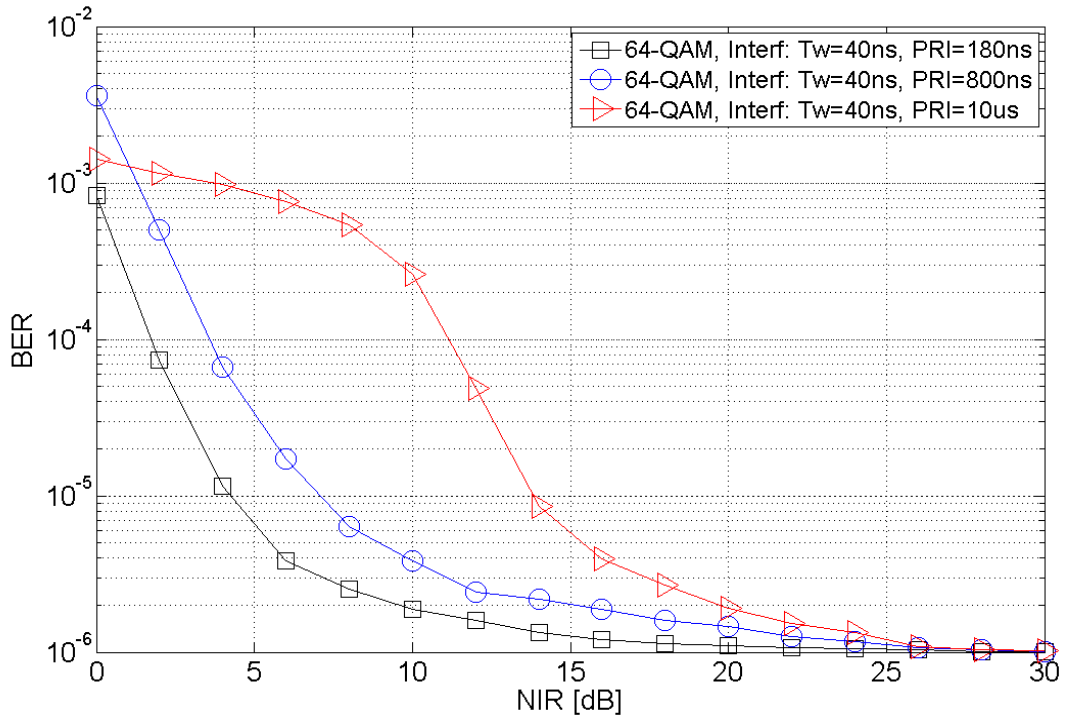


(a) BER vs. NIR

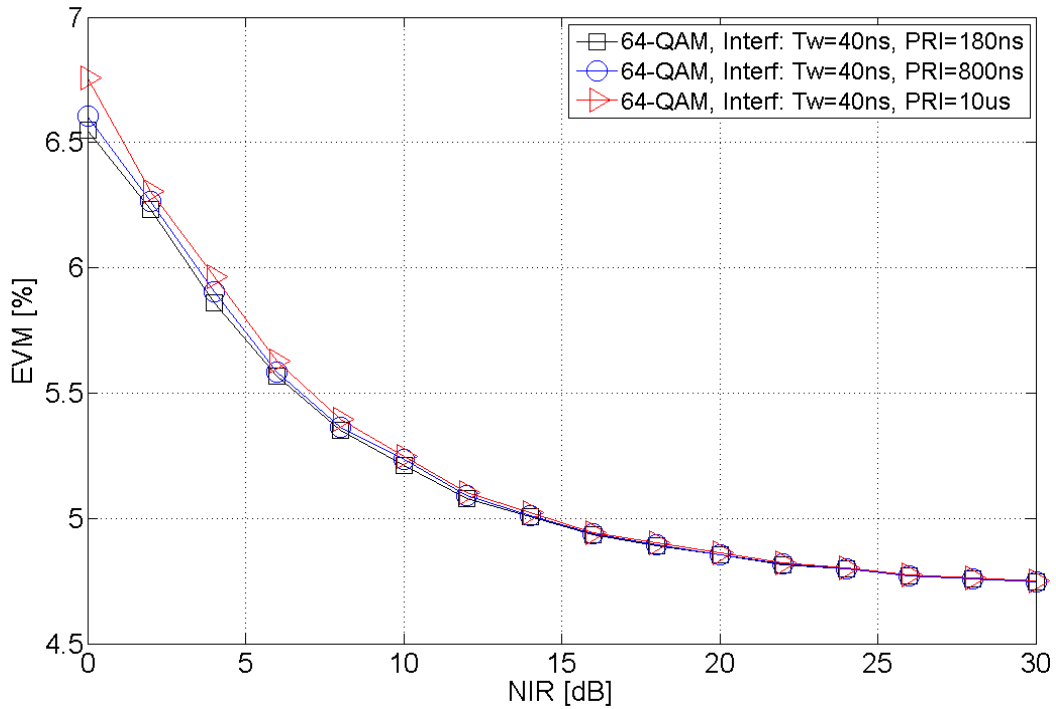


(b) EVM vs. NIR

Figure 29: BER and percentage EVM performances as a function of the NIR of a 16-QAM modulated FS system in the presence of a single UWB SRR interference with $AF=100\%$, $DC=100\%$ and $SNR = SNR_R$.



(a) BER vs. NIR



(b) EVM vs. NIR

Figure 30: BER and percentage EVM performances as a function of the NIR of a 64-QAM modulated FS system in the presence of a single UWB SRR interference with AF=100%, DC=100% and SNR = SNR_R.

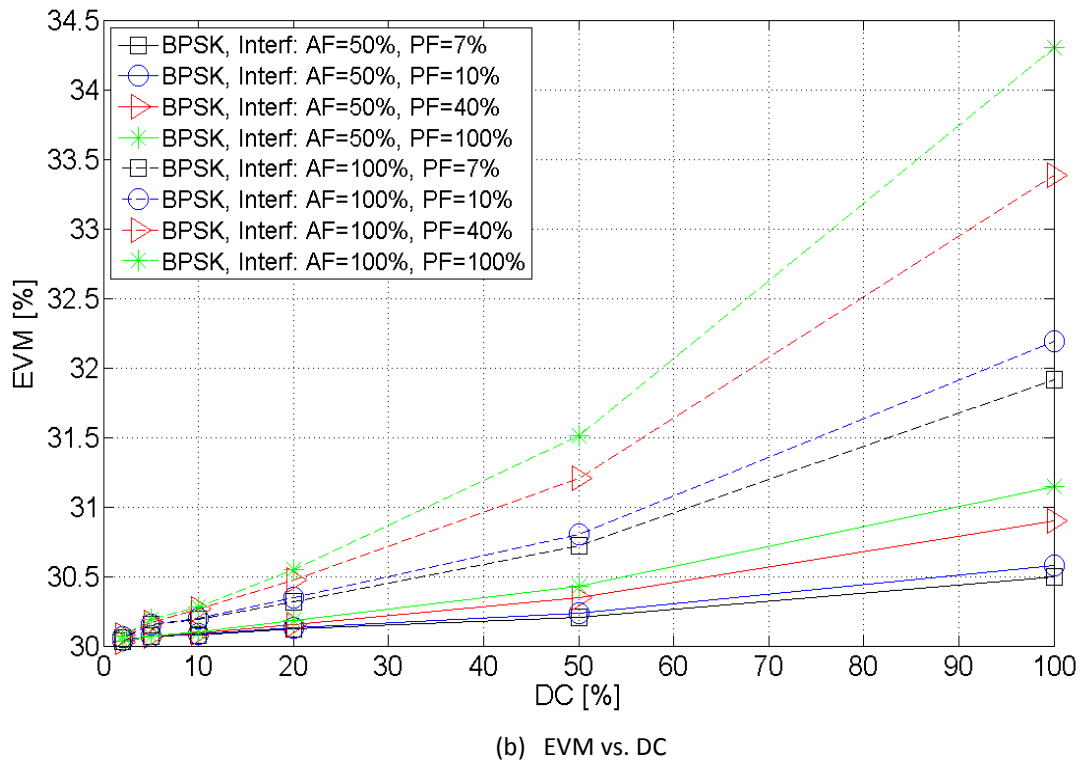
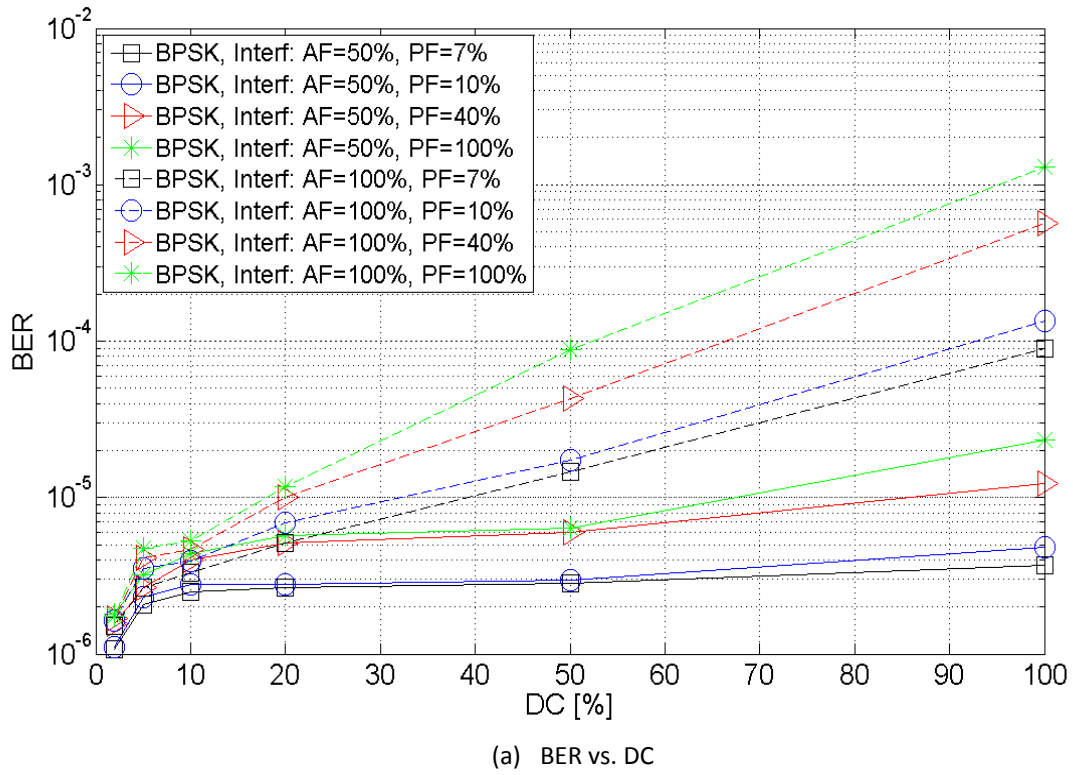
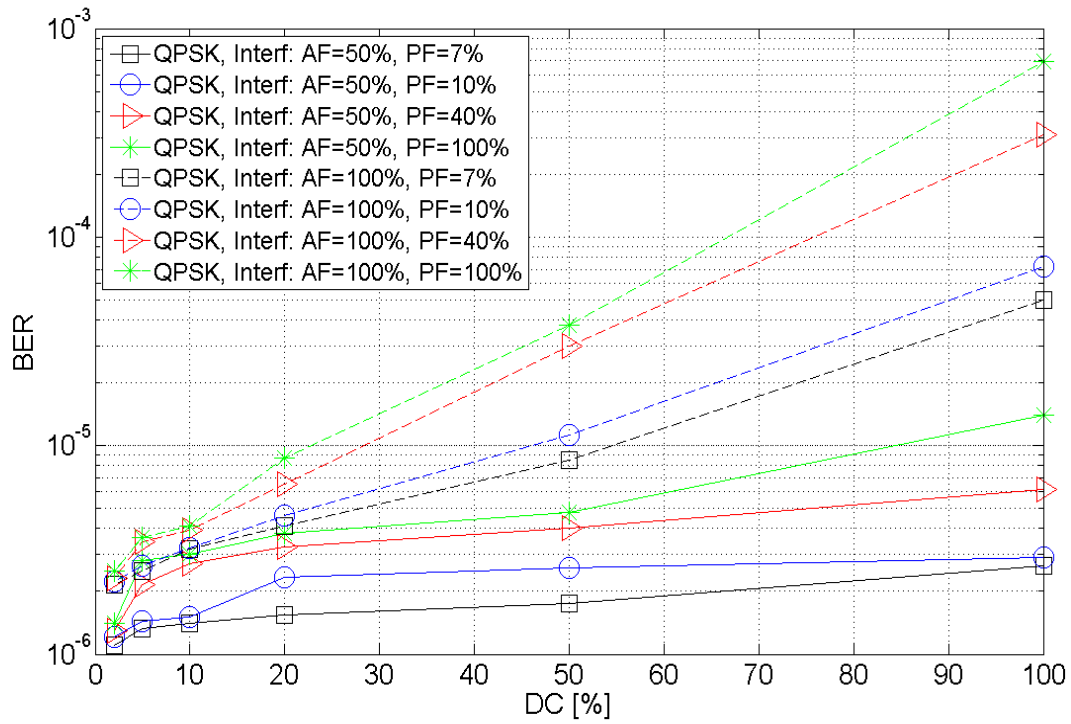
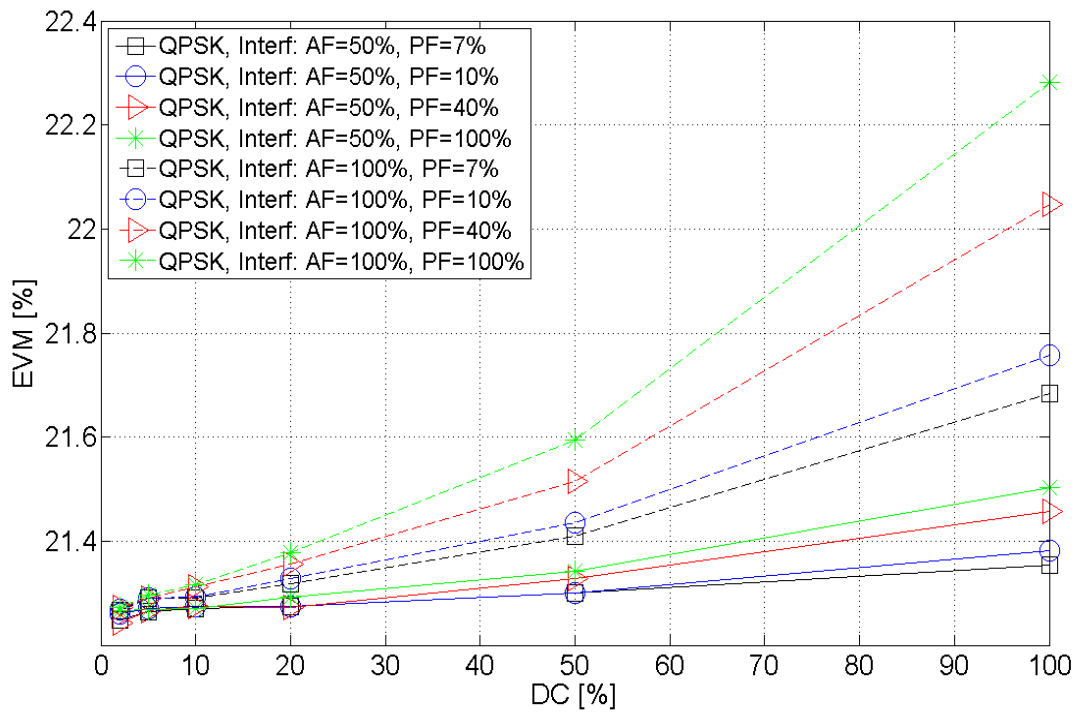


Figure 31: BER and percentage EVM performances as a function of the DC of a BPSK modulated FS system in the presence of aggregate UWB SRR interference with $PRI = 800ns$, $T_w = 40ns$ and $SNR = SNR_R$.

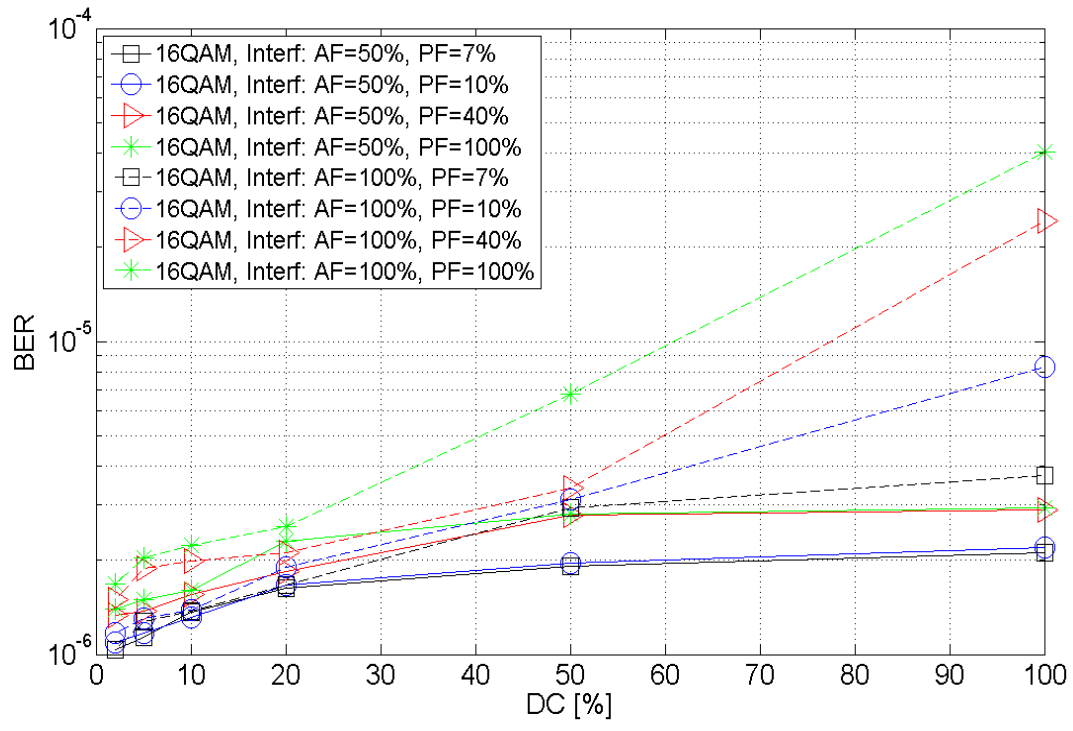


(a) BER vs. DC

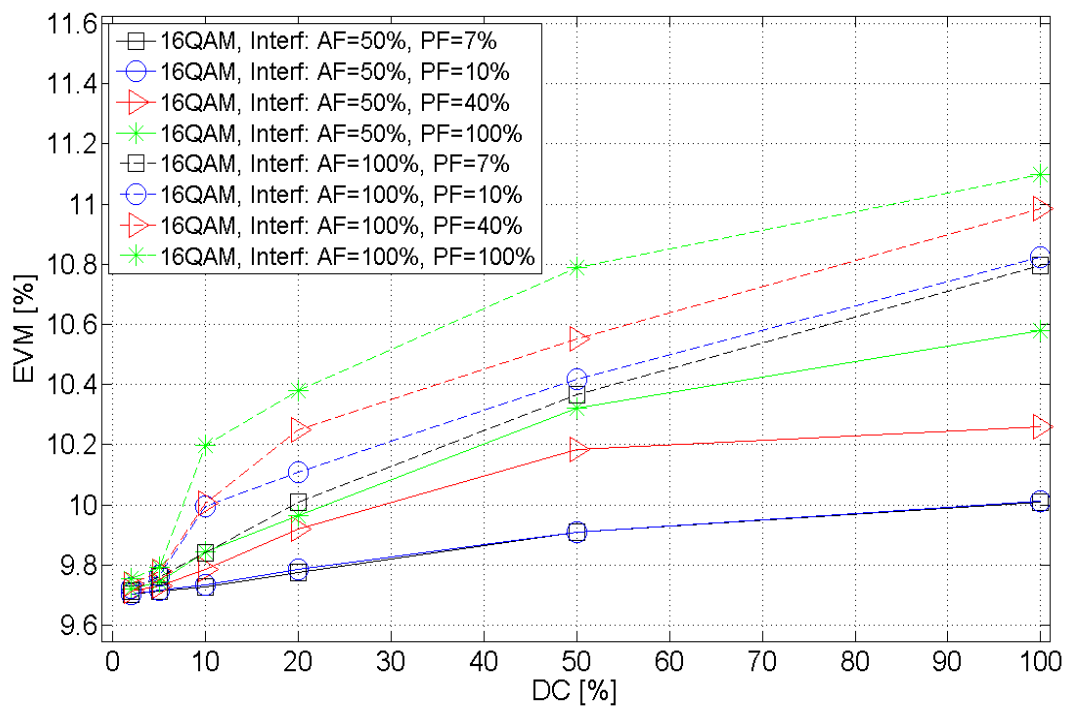


(b) EVM vs. DC

Figure 32: BER and percentage EVM performances as a function of the DC of a QPSK modulated FS system in the presence of aggregate UWB SRR interference with $PRI = 800\text{ns}$, $T_w = 40\text{ns}$ and $SNR = SNR_R$.

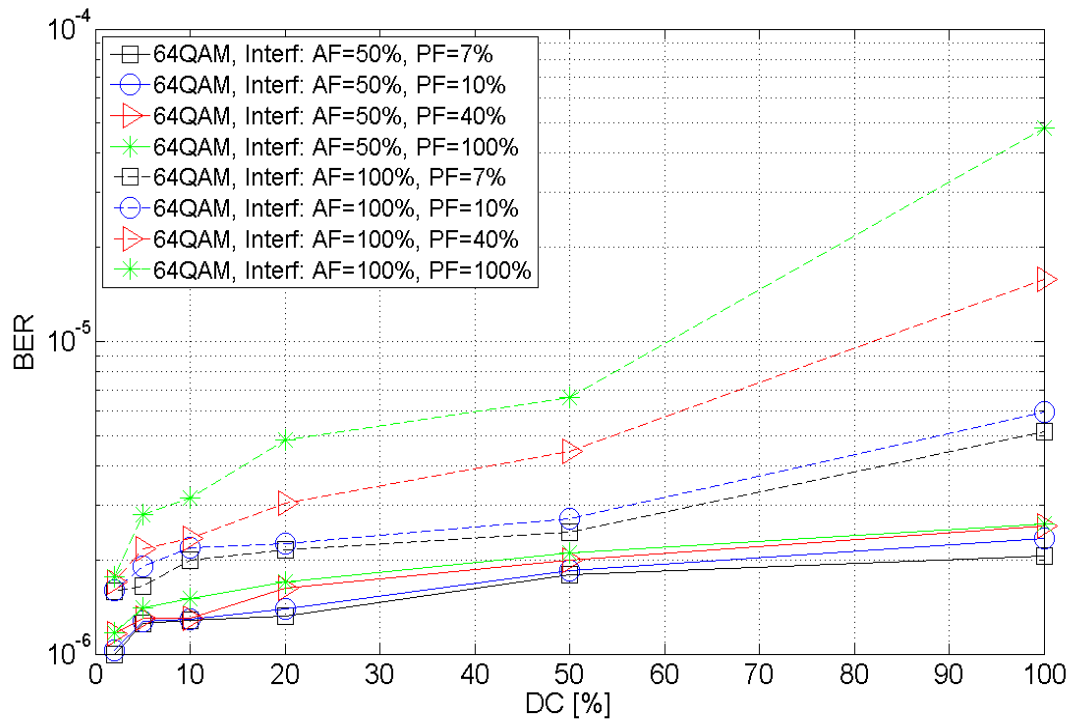


(a) BER vs. DC

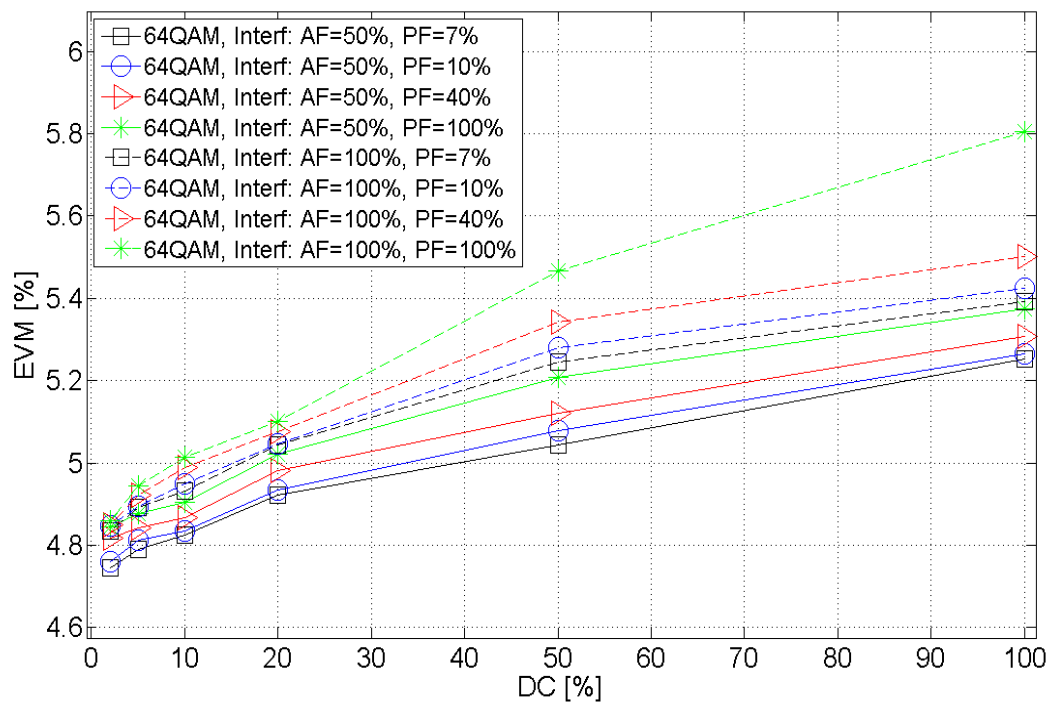


(b) EVM vs. DC

Figure 33: BER and percentage EVM performances as a function of the DC of a 16-QAM modulated FS system in the presence of aggregate UWB SRR interference with $PRI = 800\text{ns}$, $T_w = 40\text{ns}$ and $SNR = SNR_R$.

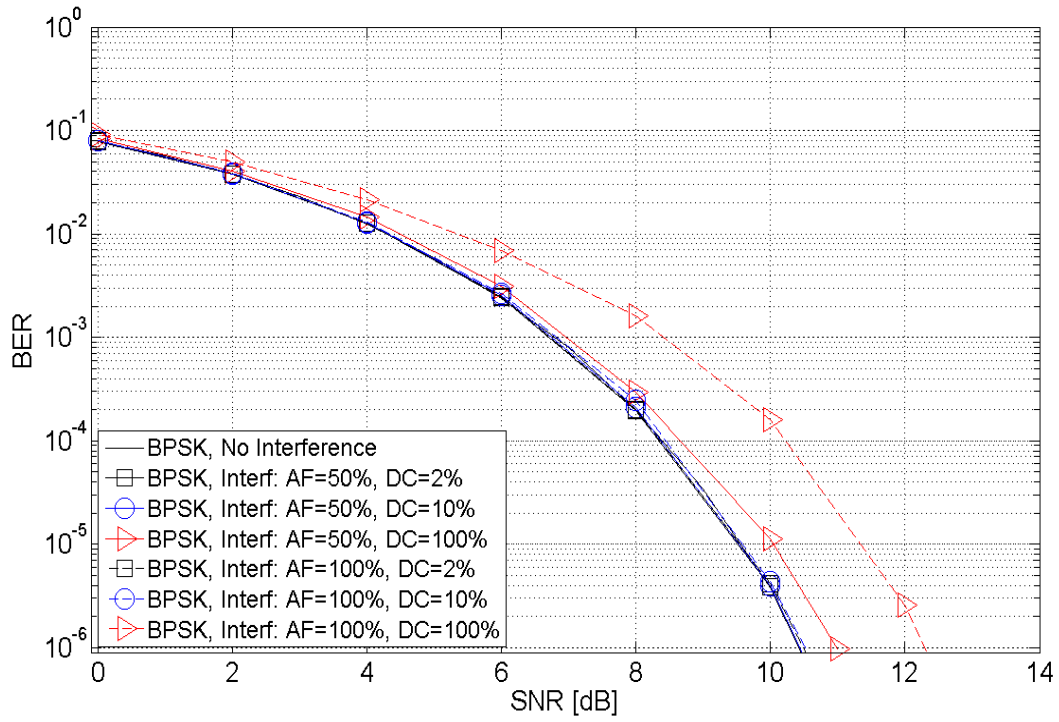


(a) BER vs. DC

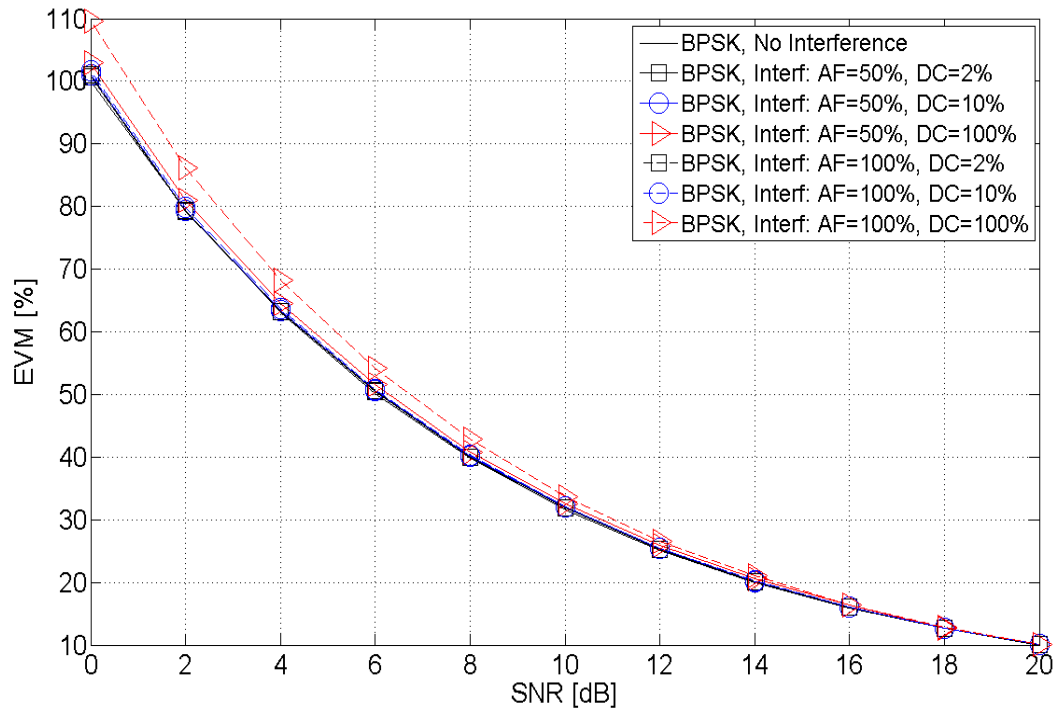


(b) EVM vs. DC

Figure 34: BER and percentage EVM performances as a function of the DC of a 64-QAM modulated FS system in the presence of aggregate UWB SRR interference with PRI = 800ns, $T_w = 40$ ns and SNR = SNR_R..



(a) BER vs. SNR



(b) EVM vs. SNR

Figure 35: BER and percentage EVM performances as a function of the SNR of a BPSK modulated FS system in the presence of aggregate UWB SRR interference with $PRI = 800ns$, $T_w = 40ns$ and $PF = 7\%$.

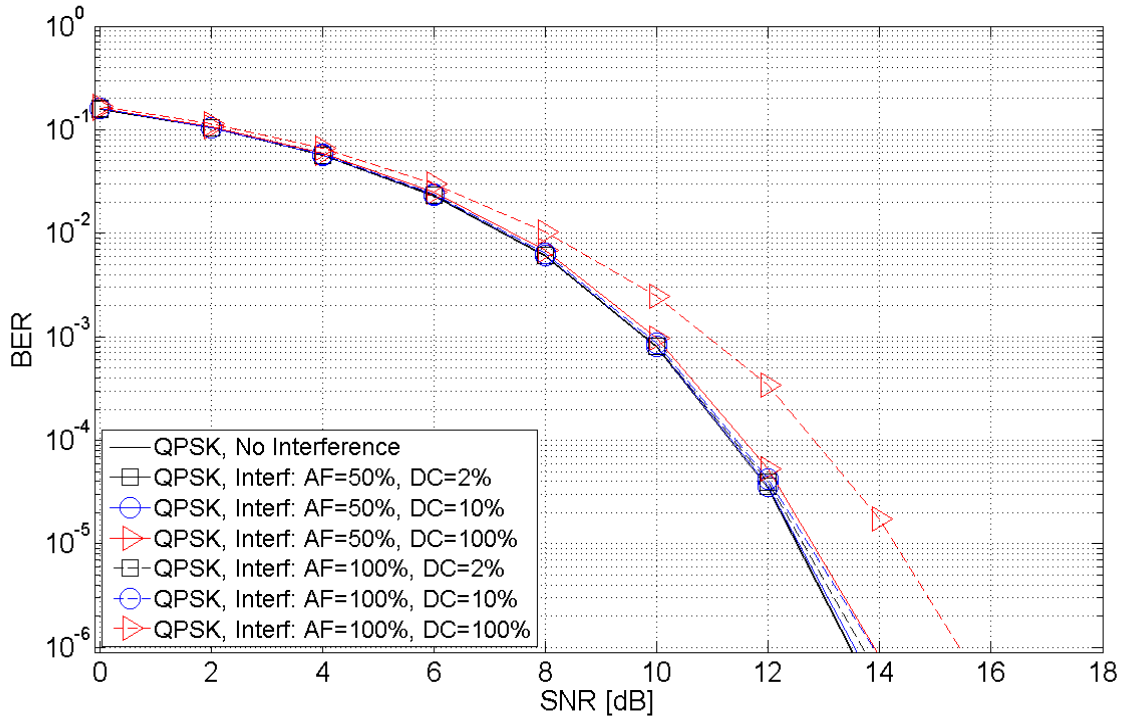


Figure 36: BER performance as a function of the SNR of a QPSK modulated FS system in the presence of aggregate UWB SRR interference with $PRI = 800ns$, $T_w = 40ns$ and $PF = 7\%$.

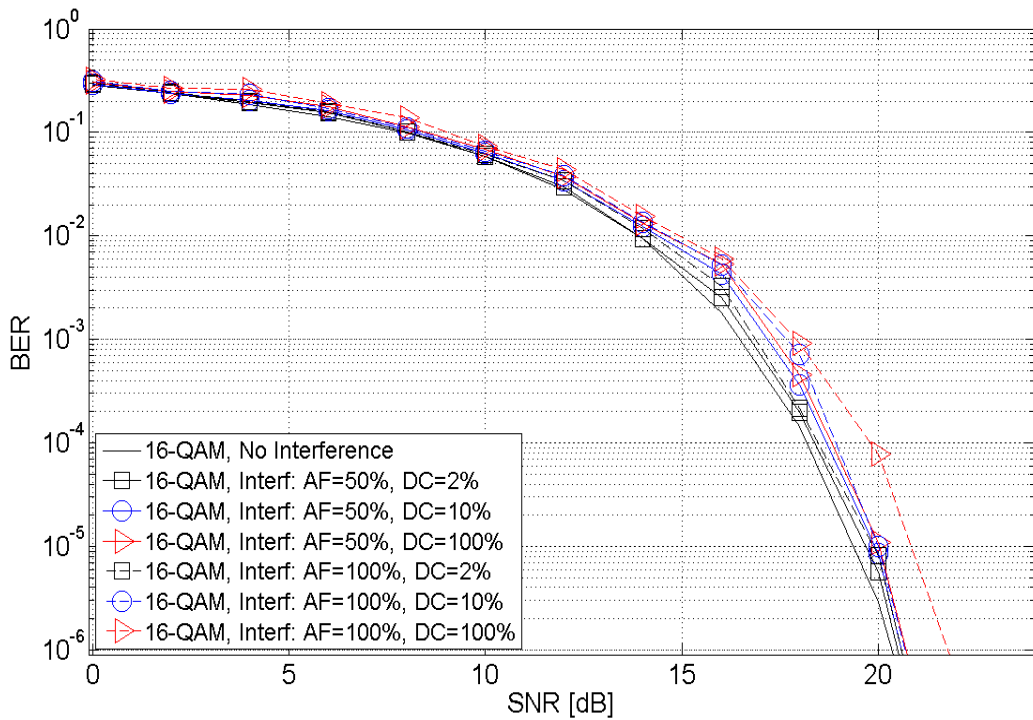


Figure 37: BER performance as a function of the SNR of a 16-QAM modulated FS system in the presence of aggregate UWB SRR interference with $PRI = 800ns$, $T_w = 40ns$ and $PF = 7\%$.

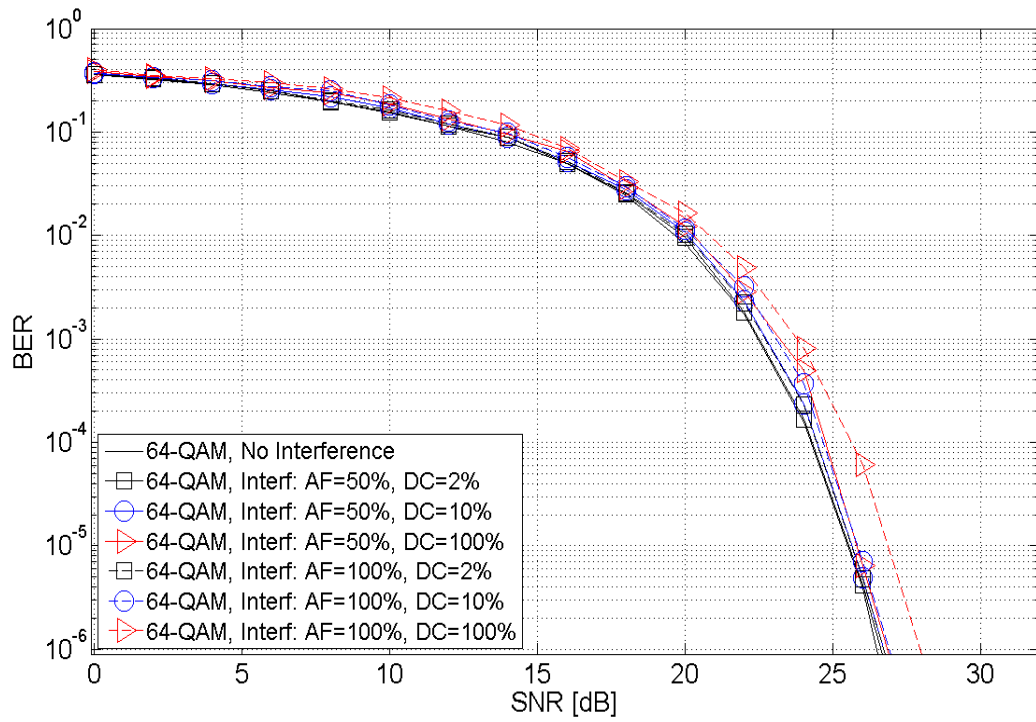
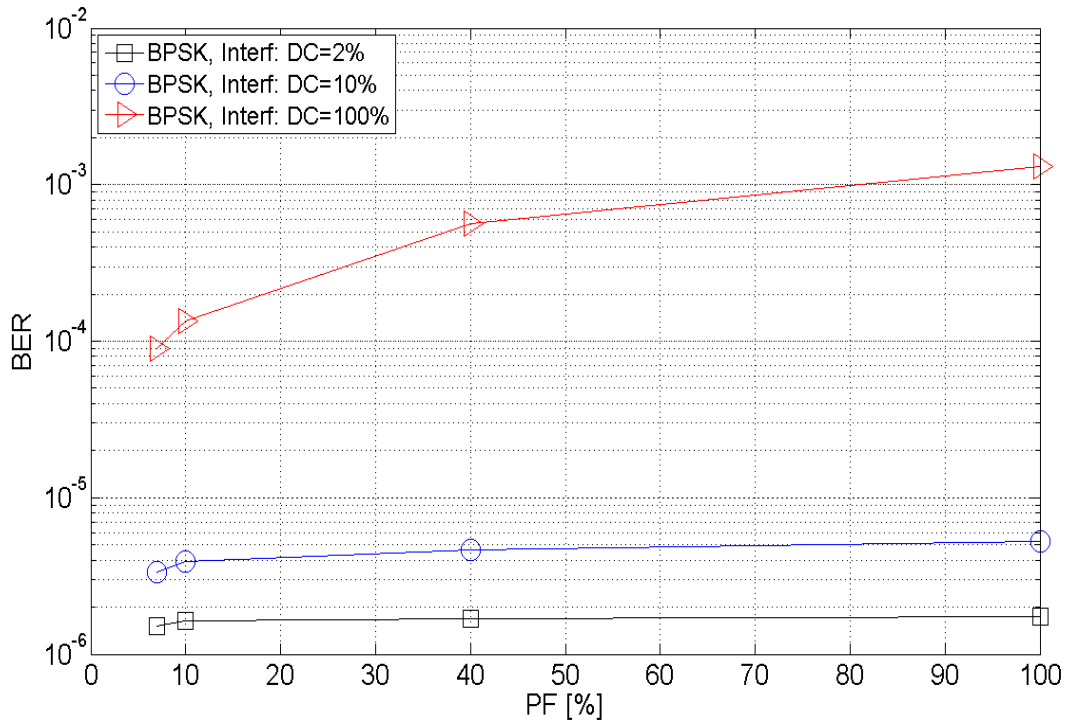
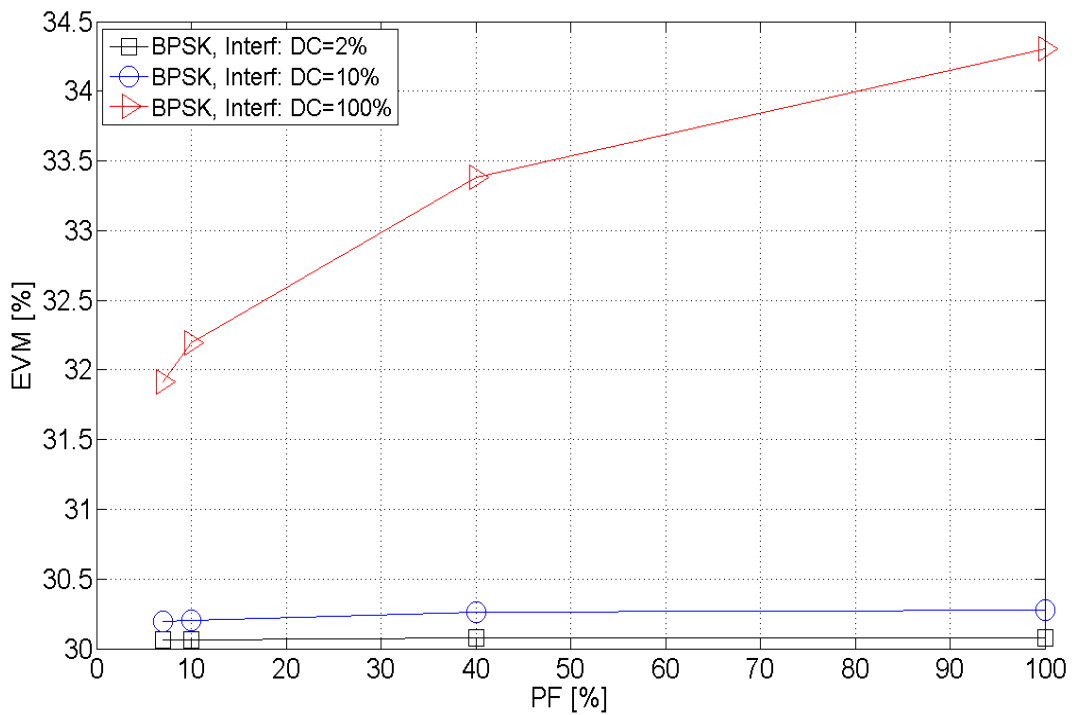


Figure 38: BER performance as a function of the SNR of a 64-QAM modulated FS system in the presence of aggregate UWB SRR interference with PRI = 800ns, $T_w = 40$ ns and PF = 7%.

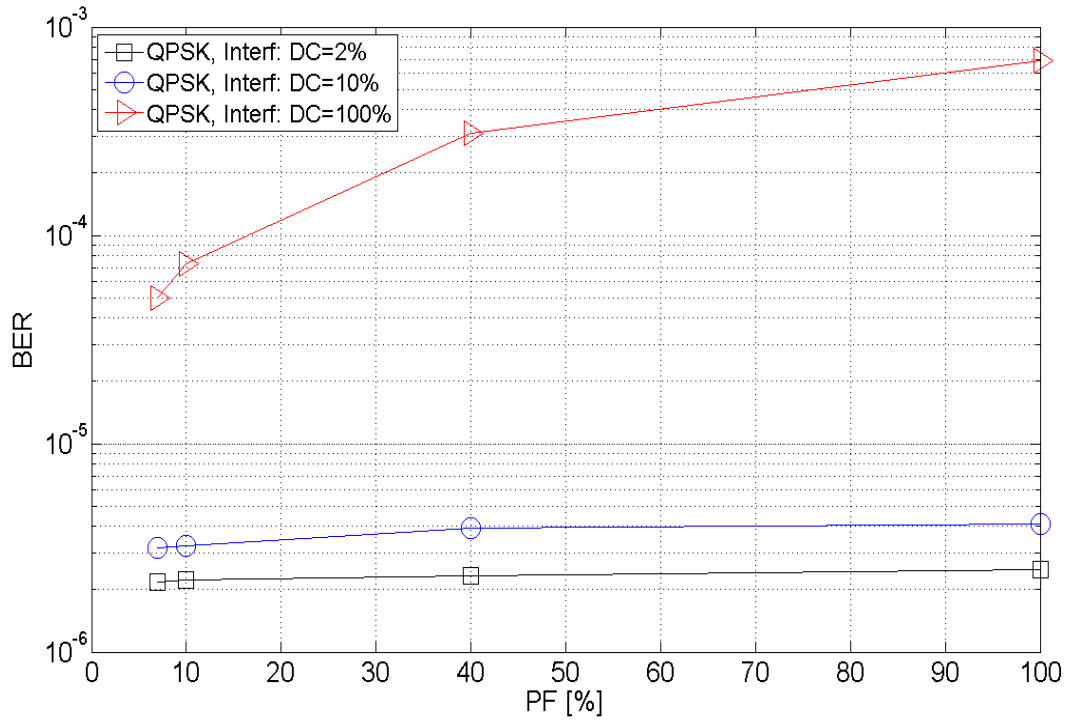


(a) BER vs. PF

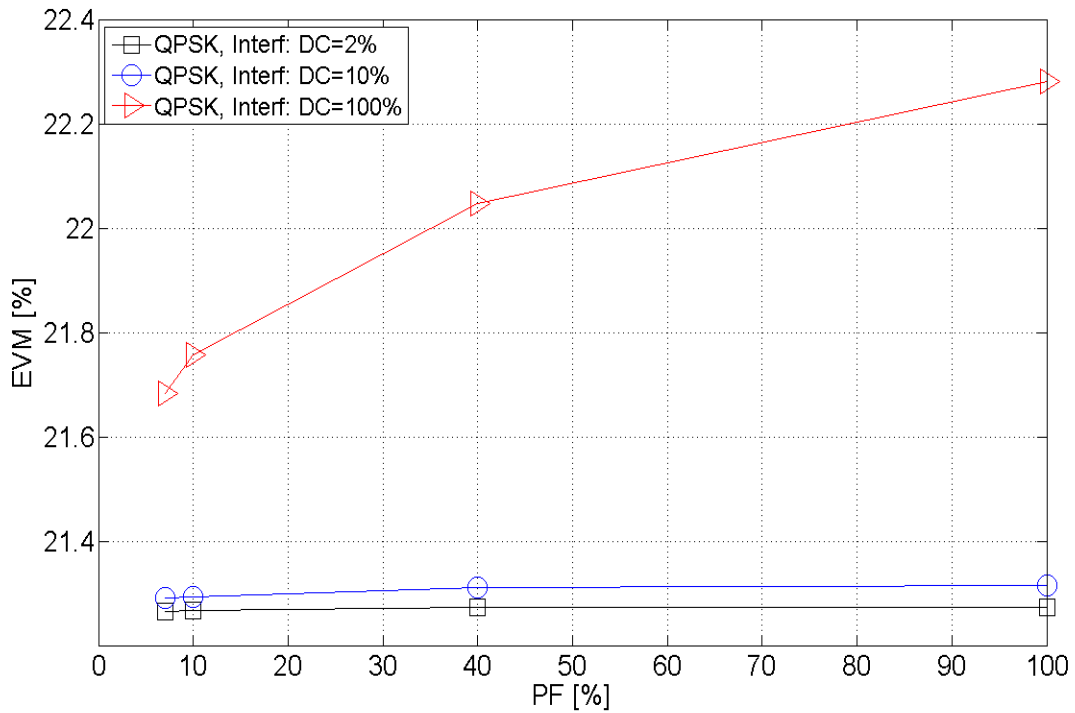


(b) EVM vs. PF

Figure 39: BER and percentage EVM performances as a function of the PF of a BPSK modulated FS system in the presence of aggregate UWB SRR interference with $PRI = 800\text{ns}$, $T_w = 40\text{ns}$, $AF = 100\%$ and $SNR = SNR_R$.

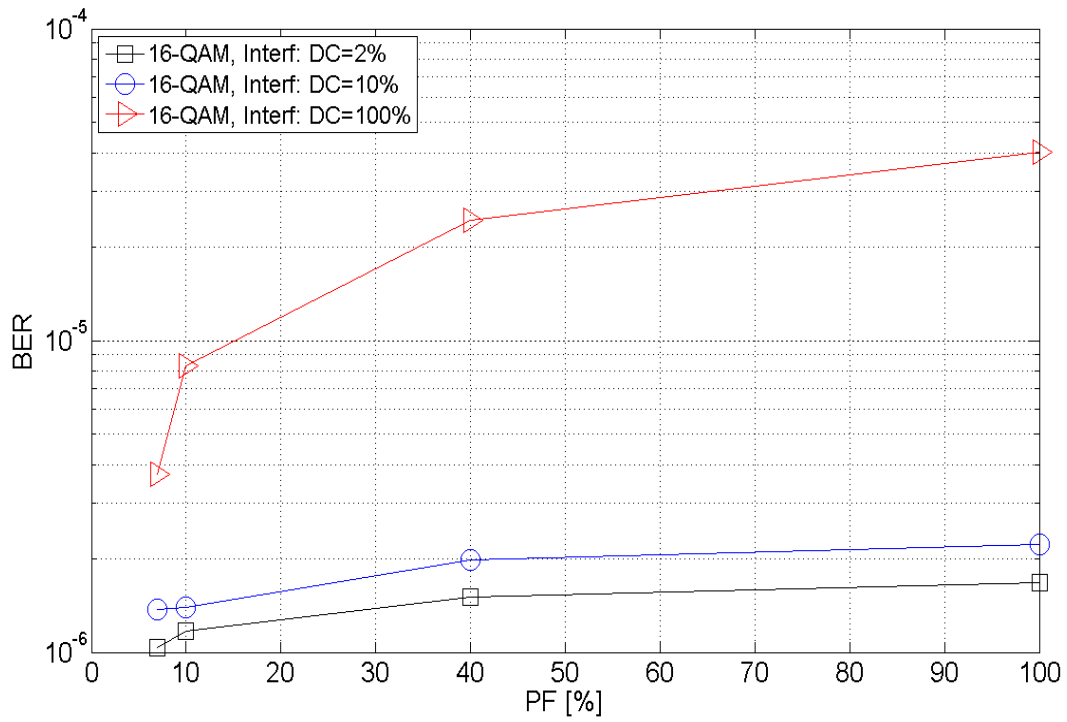


(a) BER vs. PF

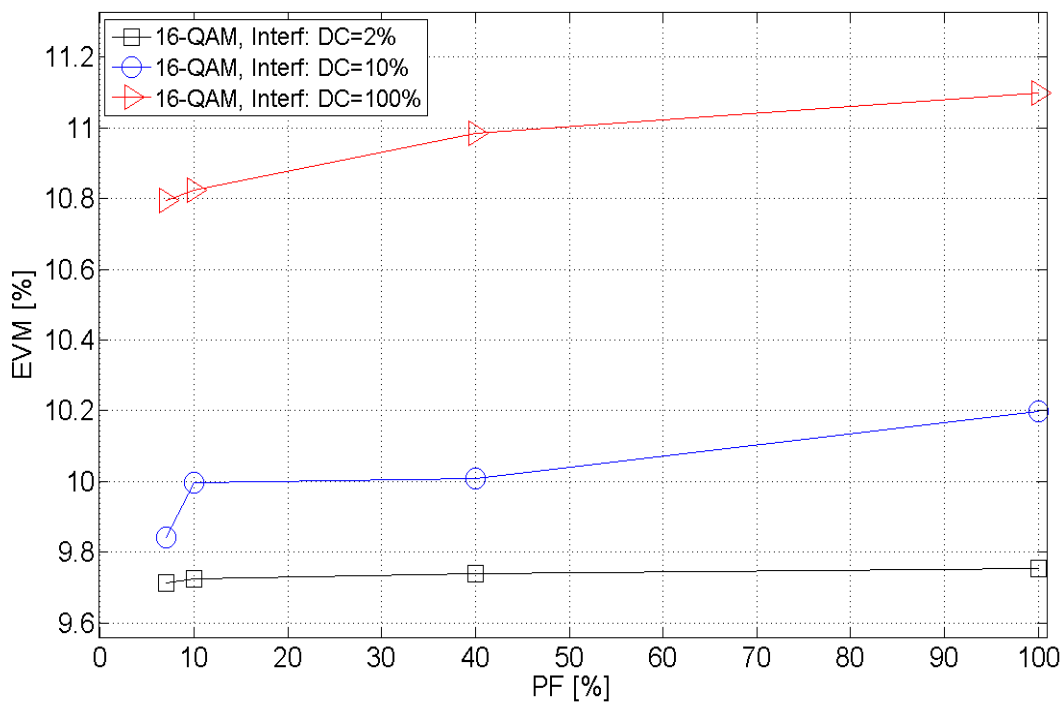


(b) EVM vs. PF

Figure 40: BER and percentage EVM performances as a function of the PF of a QPSK modulated FS system in the presence of aggregate UWB SRR interference with PRI = 800ns, $T_w = 40$ ns, AF = 100% and SNR = SNR_R.

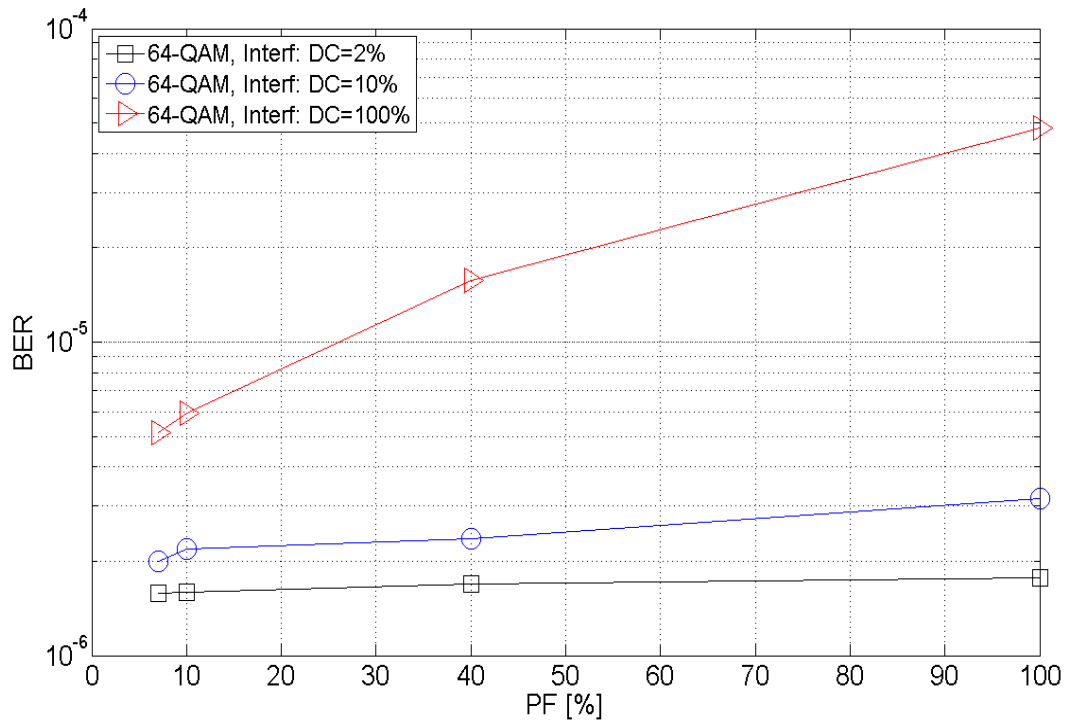


(a) BER vs. PF

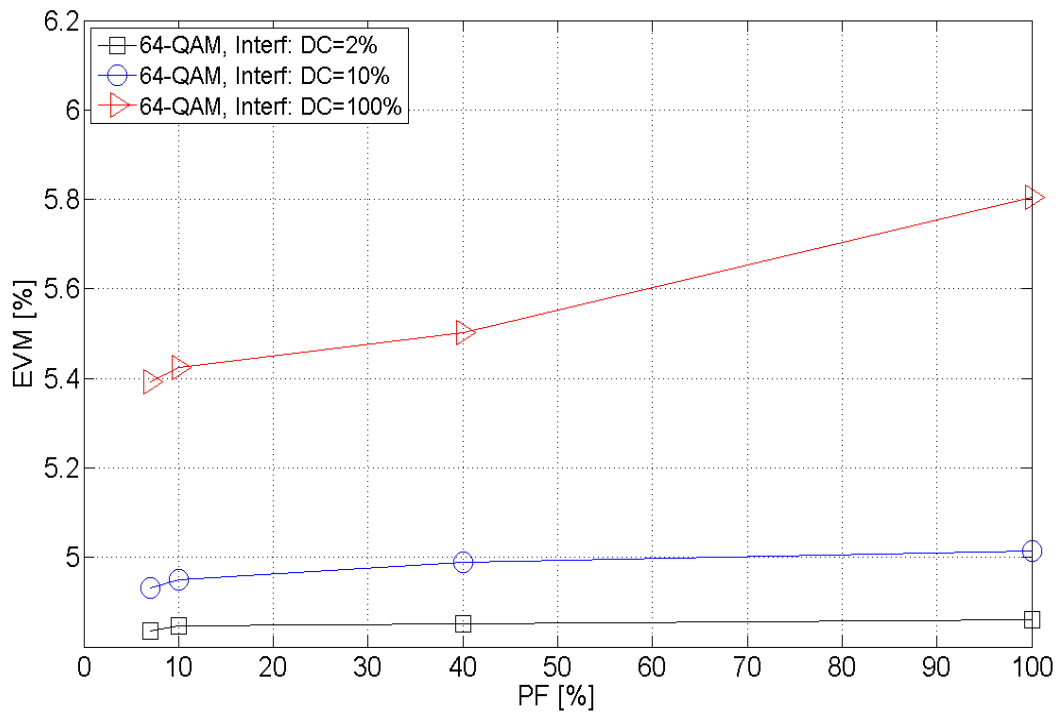


(a) EVM vs. PF

Figure 41: BER and percentage EVM performances as a function of the PF of a 16-QAM modulated FS system in the presence of aggregate UWB SRR interference with $PRI = 800ns$, $T_w = 40ns$, $AF = 100\%$ and $SNR = SNR_R$.

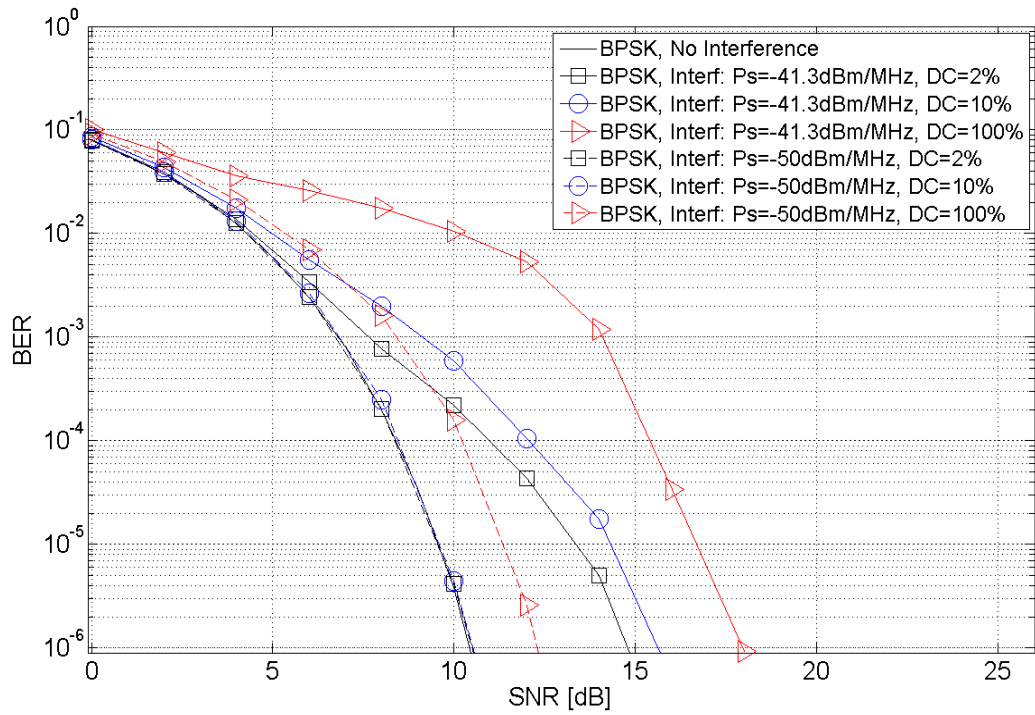


(a) BER vs. PF

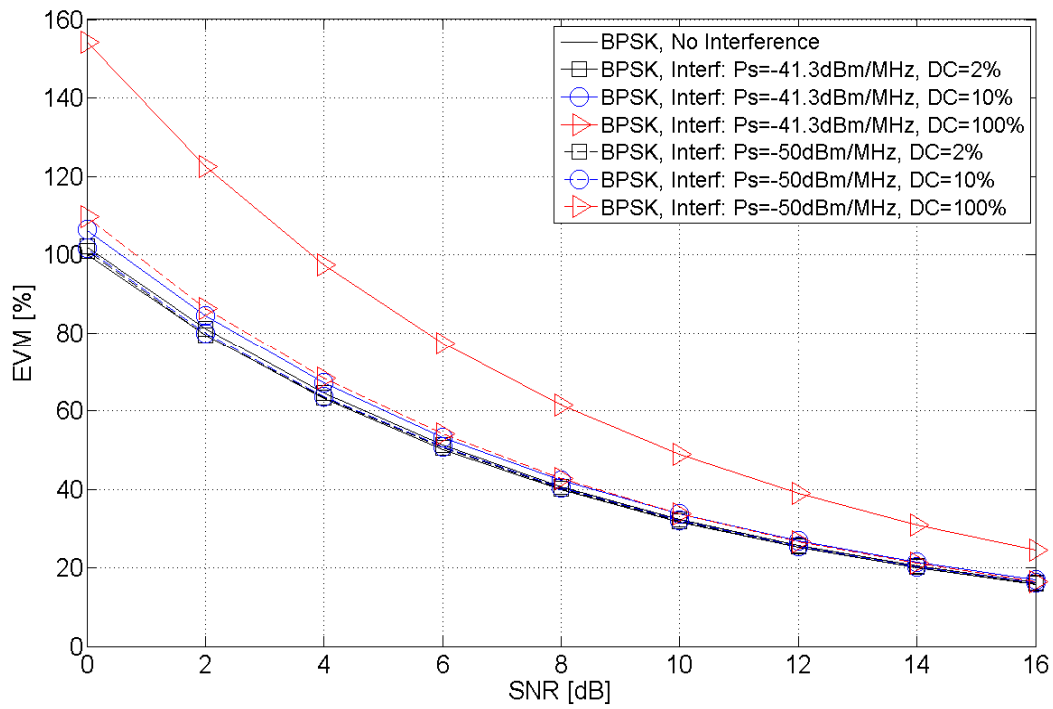


(b) EVM vs. PF

Figure 42: BER and percentage EVM performances as a function of the PF of a 64-QAM modulated FS system in the presence of aggregate UWB SRR interference with $PRI = 800ns$, $T_w = 40ns$, $AF = 100\%$ and $SNR = SNR_R$.

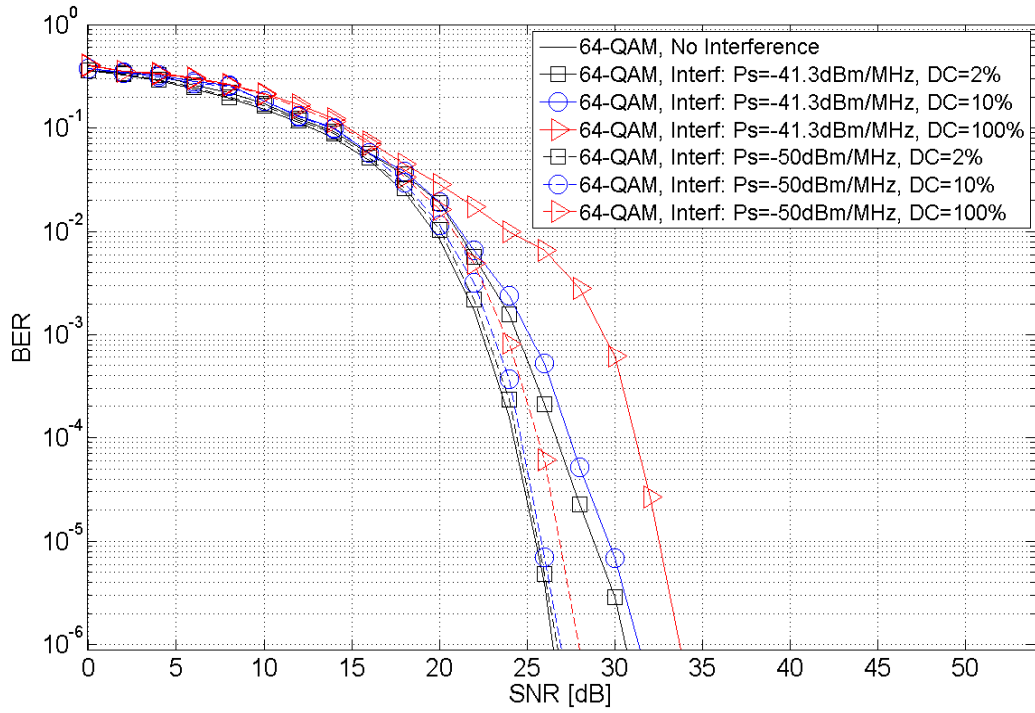


(a) BER vs. SNR

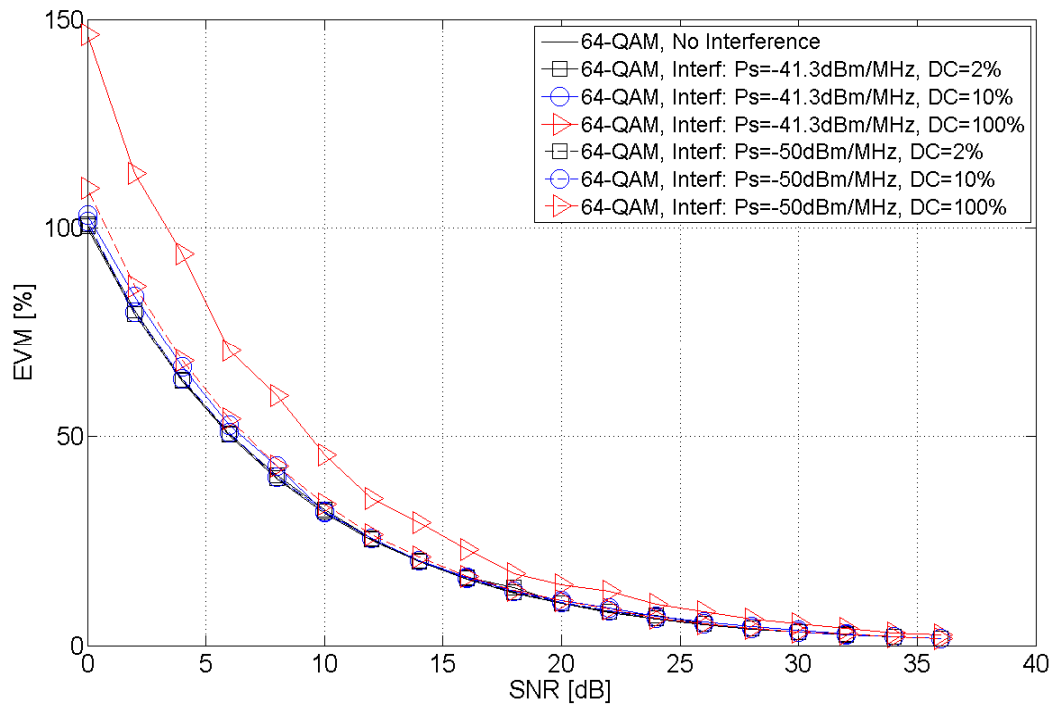


(b) EVM vs. SNR

Figure 43: BER and percentage EVM performances as a function of the SNR of a BPSK modulated FS system in the presence of aggregate UWB SRR interference with $PRI = 800ns$, $T_w = 40ns$, $PF = 7\%$ and $AF = 100\%$.



(a) BER vs. SNR



(b) EVM vs. SNR

Figure 44: BER and percentage EVM performances as a function of the SNR of a 64-QAM modulated FS system in the presence of aggregate UWB SRR interference with $PRI = 800$ ns, $T_w = 40$ ns, $PF = 7\%$ and $AF = 100\%$.

References

Normative references

- [1] EC Decision 2005/50/EC "COMMISSION DECISION of 17 January 2005 on the harmonisation of the 24 GHz range radio spectrum band for the time-limited use by automotive short-range radar equipment in the Community"
- [2] EC Decision 2004/545/EC "COMMISSION DECISION of 8 July 2004 on the harmonisation of radio spectrum in the 79 GHz range for the use of automotive short-range radar equipment in the Community"
- [3] CEPT Report 37 "Report from CEPT to the European Commission in response to Part 2 of the Mandate on "Automotive Short-Range Radar systems (SRR)", Final Report on 25 June 2010"
- [4] ETSI TR 102 664 V1.2.1 (2010-04) "Electromagnetic compatibility and Radio spectrum Matters (ERM); Road Transport and Traffic Telematics (RTTT); Short range radar to be used in the 24 GHz to 27,5 GHz band; System Reference Document"
- [5] CEPT Report 36 "Report from CEPT to the European Commission in response to Part 1 of the Mandate to CEPT on Automotive Short-Range Radar systems (SRR), Final Report on 25 June 2010"
- [6] Draft ETSI EN 302 697-1 V1.1.1rev1 (2010-05) "Electromagnetic compatibility and Radio spectrum Matters (ERM); Road Transport and Traffic Telematics (RTTT). Short Range Radar equipment operating in the 24.05 to 27.5 GHz band for UWB Short Range Radar Part 1: Technical characteristics and test methods"
- [7] ETSI EN 302 217-2-1 V1.3.1 (2010-01) "Fixed Radio Systems; Characteristics and requirements for point-to-point equipment and antennas; Part 2-1: System-dependent requirements for digital systems operating in frequency bands where frequency co-ordination is applied"
- [8] Draft ECC Report 158 "The Impact of 26 GHz SRR Applications Using Ultra-Wideband (UWB) Technology on Radio Services"
- [9] ITU-R SM.2057 "Studies related to the impact of devices using ultra-wideband technology on radiocommunication services", p. 394-431
- [10] Ægis Systems Limited "Sharing Between UWB Automotive Radars and FS Links at 24 GHz", Radiocommunications Agency, 1414/UWB-R/R/4, 16th August 2002
- [11] ITU-R SM.1755T "Characteristics of ultra-wideband technology"
- [12] J. G. Proakis, *Digital Communications*, McGraw-Hill, New York, NY, USA, 5th Edition 2008

Informative references

- [i.1] ECC Report 23 “Compatibility of Automotive Collision Warning Short Range Radar Operating at 24 GHz with FS, EESS And Radio Astronomy, Cavtat, May 2003”
- [i.2] CEPT/ERC/REC 70-03 “ERC Recommendation 70-03 (Tromsø 1997 and subsequent amendments) Relating To The Use Of Short Range Devices (SRD), Version of 6 October 2010”
- [i.3] ECC Report 46 “Immunity of 24 GHz automotive SRRs operating on a non-interference and non-protected basis from emissions of the Primary Fixed Service operating in the 23 GHz And 26 GHz frequency bands, Galati, May 2004”
- [i.4] CEPT/ERC/REC 13-04 E ” CEPT/ERC/RECOMMENDATION 13-04 E (Tallin 1998), Preferred Frequency Bands for Fixed Wireless Access in the Frequency Range between 3 And 29.5 GHz”
- [i.5] CEPT T/R 13-02 “Recommendation T/R 13-02 (Montreux 1993, amended Tromsø, May 2010), Preferred Channel Arrangements For Fixed Service Systems In The Frequency Range 22.0 - 29.5 GHz”
- [i.6] ECC Decision 04 03 “ECC Decision of 19 March 2004 on the frequency band 77 – 81 GHz to be designated for the use of Automotive Short Range Radars, (ECC/DEC/(04)03)”
- [i.7] ECC Decision 04 10 “ECC Decision of 12 November 2004 on the frequency bands to be designated for the temporary introduction of Automotive Short Range Radars (ECC/DEC/(04)10)”
- [i.8] ECC(04)053Rev1 Annex 5 “Report from CEPT to the European Commission under Mandate to CEPT to harmonise radio spectrum to facilitate a coordinated EU introduction of Automotive Short Range Radar systems, Gothenburg, 5-9 July 2004”
- [i.9] RSCOM08-81 “Opinion of the RSC, Final and adopted Mandate to CEPT to undertake Technical studies on automotive short-range radar systems (SRR), Brussels, 7 November 2008”
- [i.10] RSCOM10-46 “Working Document, Review of the 24 GHz Decision for short-range radar applications 2005/50/EC - the way forward, Brussels, 22 September 2010”
- [i.11] ITU-R SM.1756 “Framework for the introduction of devices using ultra-wideband technology”
- [i.12] ITU-R SM.1757 “Impact of devices using ultra-wideband technology on systems operating within radiocommunication services”
- [i.13] ITU-R P.530-13 “Propagation data and prediction methods required for the design of terrestrial line-of-sight systems”
- [i.14] ITU-R F.1094-2 “Maximum allowable error performance and availability degradations to digital fixed wireless systems arising from radio interference from emissions and radiations from other sources”
- [i.15] ITU-R F748 “Radio-frequency arrangements for systems of the fixed service operating in the 25, 26 and 28 GHz bands”
- [i.16] ITU-R F.758-4 “Considerations in the development of criteria for sharing between the fixed service and other services”
- [i.17] ITU-R F.699-7 “Reference radiation patterns for fixed wireless system antennas for use in coordination studies and interference assessment in the frequency range from 100 MHz to about 70 GHz”
- [i.18] ITU-R F.1245-1 “Mathematical model of average and related radiation patterns for line-of-sight point-to-point radio-relay system antennas for use in certain coordination studies and interference assessment in the frequency range from 1 GHz to about 70 GHz”

- [i.19] ETSI TR 102 982 V1.2.1 (2002-07) "Electromagnetic compatibility and Radio spectrum Matters (ERM); Radio equipment to be used in the 24 GHz band; System Reference Document for Short Range Radar"
- [i.20] Draft ETSI TR 102 892 V1.1.1_012 (2010-11) "Electromagnetic compatibility and Radio spectrum Matters (ERM); SRD radar equipment using Wideband Low Activity Mode (WLAM) and operating in the frequency range from 24,05 GHz to 24,50 GHz; System Reference Document"
- [i.21] ETSI EN 302 288-1 V1.4.1 (2009-01) "Electromagnetic compatibility and Radio spectrum Matters (ERM); Short Range Devices; Road Transport and Traffic Telematics (RTTT); Short range radar equipment operating in the 24 GHz range; Part 1: Technical requirements and methods of measurement"
- [i.22] ETSI EN 302 288-2 V1.3.2 (2009-01) "Electromagnetic compatibility and Radio spectrum Matters (ERM); Short Range Devices; Road Transport and Traffic Telematics (RTTT); Short range radar equipment operating in the 24 GHz range; Part 2: Harmonized EN covering the essential requirements of article 3.2 of the R&TTE Directive"
- [i.23] FCC 15.515 "Technical requirements for vehicular radar systems"
- [i.24] M.Z. Win and R.A. Scholtz, "Ultra-wide bandwidth time-hopping spread-spectrum impulse fir wireless multiple-access communication", IEEE Transactions on Communications, 48:679-689, April 2000

European Commission

EUR 24833 EN – Joint Research Centre – Institute for the Protection and Security of the Citizen

Interference from Low-Duty Cycle 26 GHz Automotive Short Range Radar (SRR)

D.Fuehrer, E. Cano-Pons, J. Fortuny-Guasch

Luxembourg: Publications Office of the European Union

2011 – 57 pp. – 21 x 29.7 cm

EUR – Scientific and Technical Research series – ISSN 1018-5593 (print), ISSN 1831-9424 (online)

ISBN 978-92-79-20396-1 (print)

ISBN 978-92-79-20397-8 (pdf)

doi:10.2788/24368

Abstract

Currently, there are two frequency bands allocated to Ultra-Wideband (UWB) automotive short range radar (SRR) equipment in Europe. In its Decision 2005/50/EC of 17 January 2005 [1] the European Commission (EC) designated the frequency band 21.65-26.65 GHz (referred to as the “24 GHz band”) for use until mid 2013. The frequency band 77-81 GHz (the “79 GHz band”) has been designated and made available for permanent usage by EC Decision 2004/545/EC of 8 July 2004 [2] In order to ease the transition from 24 GHz to 79 GHz technology the EC considers authorizing the use of a band in the 24 GHz range for SRR beyond 2013. In Report 37 of the European Conference of Postal and Telecommunications Administrations (CEPT) [3] which was prepared in response to the “SRR mandate 2” issued by the EC to the CEPT it is proposed to allocate the frequency band 24.25 – 27.50 GHz (the “26 GHz band”) to SRR and reduce the risk of interference to licensed services operating in the same band through lower transmit power limits and low duty cycle (LDC) operation. As this proposal was not accepted the discussion now centres on the frequency band 24.25 – 26.65 GHz (the “revised 26 GHz band”).

The objective of this report is to complement the very detailed and comprehensive compatibility studies that have been undertaken by CEPT, ITU-R, ETSI, and other institutions over the past years by evaluating the impact of LDC on the level of interference generated by automotive UWB SRR systems in the revised 26 GHz band. In particular, the impact on digitally modulated single carrier signals as used by licensed microwave fixed wireless links is investigated. The conclusions drawn in this report will hopefully be useful for defining the future regulation for automotive SRR in the European Union.

How to obtain EU publications

Our priced publications are available from EU Bookshop (<http://bookshop.europa.eu>), where you can place an order with the sales agent of your choice.

The Publications Office has a worldwide network of sales agents. You can obtain their contact details by sending a fax to (352) 29 29-42758.

The mission of the JRC is to provide customer-driven scientific and technical support for the conception, development, implementation and monitoring of EU policies. As a service of the European Commission, the JRC functions as a reference centre of science and technology for the Union. Close to the policy-making process, it serves the common interest of the Member States, while being independent of special interests, whether private or national.

LB-NA-24833-EN-N



ISBN 978-92-79-20397-8

